Composites: Part A 147 (2021) 106443

Contents lists available at ScienceDirect

Composites Part A

journal homepage: www.elsevier.com/locate/compositesa

Review

Surface preparation strategies in secondary bonded thermoset-based composite materials: A review

Arief Yudhanto [a], Marco Alfano [b], Gilles Lubineau [a,*]

[a] King Abdullah University of Science and Technology (KAUST), Physical Science and Engineering Division, COHMAS Laboratory, Thuwal 23955-6900, Saudi Arabia

[b] Department of Mechanical and Mechatronics Engineering, University of Waterloo, 200 University Avenue West, Waterloo, Ontario N2L 3G1, Canada

ARTICLE INFO

Keywords:
A. Polymer–matrix composites (PMCs)
B. Mechanical properties
E. Joining/joints
E. Surface treatments

ABSTRACT

A considerable weight reduction in thermoset-based composite is attained by replacing mechanical fasteners with a structural adhesive during the secondary bonding. The quality of this adhesively-bonded joint greatly depends on the surface preparation strategies applied to the mating composites as they influence the surface morphology, topography, *interface* composition, and mechanical performance of the adherend–adhesive *interphase*. We reviewed the recent progress of surface preparation strategies generally employed for the aerospace or automotive-grade thermoset composites (carbon/epoxy and glass/epoxy). Then, we briefly reviewed the role of each of them in promoting adhesion mechanisms, *i.e.*, mechanical interlocking, adsorption/chemical bonding, and diffusion. Subsequently, we analyzed qualitatively and quantitatively the effects on indicators associated with surface characteristics of the treated surface and mechanical performance metrics. Finally, we discussed two emerging solutions, namely substrate patterning, and adhesive tailoring. Our analysis shows that creating heterogeneity in the composite adherends or adhesive enables effective tuning of the joint performances.

1. Introduction

Fiber-reinforced laminated composites are increasingly used to manufacture aerospace or automotive structures owing to their excellent fatigue life, non-corrosive nature, and weight-saving capability [1–3]. The weight-saving capability is achieved by minimizing the use of classical mechanical fasteners (rivet, bolt) to join composite parts, which are structurally heavy, corrosive, and causing stress concentrations [4]. To replace the mechanical fasteners, bonding strategies, which contribute to the weight-saving concept, are employed, namely co-curing, co-bonding and secondary bonding [4,5] (see Fig. 1a). Co-curing refers to the combination of two uncured parts (with or without adhesive), and their subsequent curing by the same process. Co-bonding refers to the scenario where one uncured part is combined with a cured part (where adhesive may also be used), and subsequently cured by the same process. Secondary bonding corresponds to the bonding of two cured parts using a structural adhesive that is subsequently cured. Among these joining techniques, co-curing and co-bonding are mostly used in the initial stage of aircraft manufacturing, yielding good bonding properties and large structures. However, co-curing and co-bonding generally require expensive tooling. Secondary bonding, in contrast, is more versatile, as it offers faster assembly, easier handling, lower manufacturing cost, and can be implemented at the later stage of structural integration, providing more flexibility in the fabrication cycle [6,7]. Therefore, secondary bonding is quite attractive for numerous industries, as it fully unlocks both cost-effectiveness and weight-saving capability.

Historically, secondary bonding was adopted to bond metallic parts [8], *e.g.*, the rocket nozzle of MX spacecraft [9]. With the increasing use of composites in modern aircraft, secondary bonding is adopted to fabricate the stiffener-to-ribs connection in the A380 vertical/horizontal tail-plane [10]. During operation and maintenance, secondary bonding has been used as a repair scheme for damaged parts [11–13], as the secondary-bonded part exhibits a similar strength to a co-cured or co-bonded structure [14]. Albeit promising, secondary bonding considerably relies on numerous factors, *i.e.*, surface preparation/treatment, adhesive type, adherend/substrate materials, joint geometry (bondline thickness, joint configuration, overlap length), environment, and curing process [15–23]. Surface preparation is recognized to be among the most critical factors [24,23]. It largely modifies the morphology, topography and chemical composition of the mating substrates, where the contaminant removal, intermolecular interactions

* Corresponding author.
E-mail address: gilles.lubineau@kaust.edu.sa (G. Lubineau).

https://doi.org/10.1016/j.compositesa.2021.106443
Received 9 February 2021; Received in revised form 20 April 2021; Accepted 22 April 2021
Available online 24 April 2021

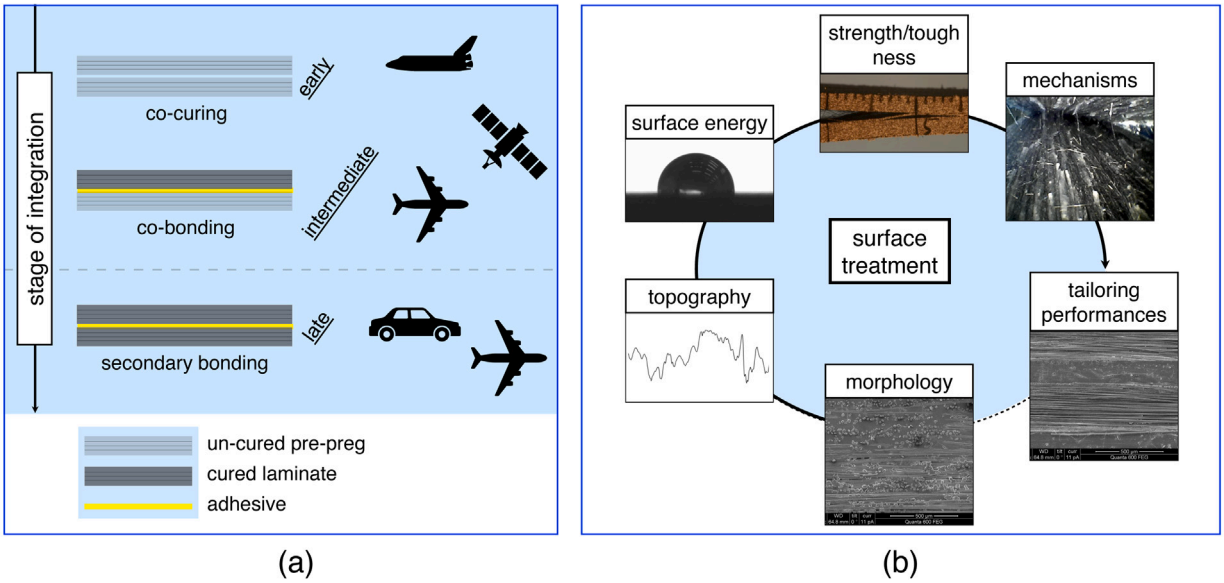

Fig. 1. (a) Schematic representation of strategies deployed for joining composite materials in aerospace, aviation and automotive industries. Because of enhanced flexibility, late integration of secondary bonding is conducive to the fabrication of modern lightweight airframes and automotive body-in-white; (b) classical chain of research and development activities carried out for the implementation and optimization of surface treatments.

(*e.g.*, physical adsorption, chemical adsorption), and mechanical interlocking of the adhesive within surface asperities are all affected. Furthermore, surface preparation eventually determines the strength and fracture toughness of bonded substrates, as well as the composite integrity [25,21]. All these surface preparation aspects (analysis of morphology, topology, surface energy, strength/toughness, toughening mechanisms, and tailoring performances) are summarized in a classical chain shown in Fig. 1b, and are subject to the exciting research and development activities.

In terms of surface preparation methods, the aerospace industry generally employs peel ply to treat a relatively large surface prior to bonding process [10,21]. The automotive industry usually adopts more delicate techniques, such as plasma [26,25,10,27] or flame [28,29], as the treated surface of these parts can be relatively small. Solvent cleaning [30,31], sanding [32], grit blasting [10,24,32], corona discharge [33], and two methods that recently received some attention, chemical functionalization [34,35] and laser irradiation [25,10,36–39], are among other employed methods.

Because surface preparation or treatment is a highly active research area, its development has been reviewed in some published studies concerning metallic and composite joints [33,40,41,15,25,42,27,31,13,39]. Several reviews focused on identifying various treatments for preparing the surface of certain materials. Critchlow and Brewis [40] identified 41 treatments for metallic bonded joints (aluminum). Wingfield [33] reviewed various treatments for thermoset or thermoplastic composites, and discussed their effects on the joint strength. Baldan [15] produced a considerably complete review of various treatments for polymers, composites, and metals, as well as their relationship with the surface energy, roughness, chemistry, strength and durability of bonded joints. The review on treatments for joining dissimilar materials is provided in Ref. [41] for titanium-composites, and Ref. [43] for aluminum-composites. More recent reviews generally focus on specific treatments for certain purposes, *e.g.*, plasma and laser treatments for adhesively bonded composite patches [25], grit blasting and plasma for composite and metal-to-composite joints [42], plasma treatments for biomedical polymers [27], and laser treatment for metal substrates [39]. These reviews emphasize that surface treatment generally modifies the surface (morphology, topography, wettability, surface energy) and mechanical (strength, toughness) characteristics. Nonetheless, increasing use of high-performance thermoset composites (carbon/epoxy, glass/epoxy) for automotive and aerospace structures demands a thorough review of treatments adopted for these materials. Such a review, however, is not available to date.

Our study reviews the recent developments in the treatments for thermoset-based composite materials (carbon/epoxy or CFRP; glass/epoxy or GFRP) used in aerospace and automotive industries. The analysis in this review is based on a mechanistic and quantitative point-of-view that clarifies the advantages and disadvantages of each technique, and how some treatments are used to activate the adhesion mechanism and to improve surface and mechanical indicators. We tabulate the relationship between adhesion mechanisms (mechanical interlocking, adsorption/chemical bonding, diffusion) and surface preparation methods, and the modification level in terms of surface and mechanical indicators derived from numerous published studies spanning the past 25 years. Furthermore, we provide an overview of modern solutions enabled by surface preparations.

This paper is organized as follows. The second section reviews the most common surface preparation strategies for thermoset-based composites, namely peel ply, solvent cleaning, detergent washing, sanding, blasting, etching (acid and base), corona discharge, plasma, flame, chemical functionalization, and laser treatments. The third section provides a possible link between surface preparation methods and adhesion mechanisms, including mechanical interlocking, adsorption/chemical bonding, and diffusion [44]. The fourth section discusses the effect of surface preparation strategies on surface indicators (*i.e.*, morphology, roughness, wettability, contact angle, surface energy, and chemistry) and mechanical indicators (*i.e.*, strength, Mode I and Mode II toughness of the joints). Finally, we highlight that, despite the importance of improving intrinsic adhesion through surface preparation, the ability to inhibit damage progression is crucial. Thus, the last section discusses modern solutions for controlling joint performance utilizing surface treatments that include methods to introduce local toughening [45–47] and novel dissipation mechanisms (*e.g.*, extrinsic toughening by ligaments) [48,49,36,37,50–53].

2. Surface preparation strategies for thermoset-based composites

2.1. Peel ply treatment

Peel ply treatment is a method for attaching and removing textured fabric on a pre-impregnated (pre-preg) composite surface before the

curing process. Peel ply has been used in industry to treat pre-preg thermoset composites (carbon/epoxy and glass/epoxy) before co-bonding or the secondary bonding process. As a surface preparation strategy, peel ply ensures good repeatability, easy application and removal, and cost effectiveness [54–57]. Two peel ply products have been employed for thermoset pre-preg: dry peel ply and wet peel ply (known as 'tear ply' with a partially cured resin [55]).

Dry peel ply is used to remove the outermost portion of the surface matrix, and replace it with a fresh, textured resin layer. This process creates a repetitive pattern on the cured surface unique to the selected textured fabric, and leaves a topology that is characterized by matrix protrusions (due to the shape of fiber tows) and arrays of trenches (due to transition between warp and weft tows, or the arrangement of individual fibers) [58,59]. This topology inherently exhibits a surface roughness, and contributes significantly to the activation of mechanical interlocking [60] that improves joint strength and toughness [61,54,62–64,59]. Factors affecting the texture and roughness are (i) peel ply material [21] with a typical layer thickness of 110–150 μm [64], such as polyamide [54,59,64,37,32], polyester [61,54,62,65,63,64], and glass [58,59,66]; (ii) woven type of peel ply, such as plain and twill [59]; (iii) tow characteristics of the woven type (for example, 3000 fibers in an individual tow; individual fiber diameter typical ranging 6–29 μm) [59,62]. Polyamide peel ply yields lower surface roughness and higher nitrogen content on the CFRP surface than polyester peel ply, thus affecting the bonding with epoxy. Consequently, the Mode I fracture toughness of polyamide treated-CFRP is 80% lower than polyester treated-CFRP [57]. The woven type and tow characteristics mostly affect the desired texture and roughness. Furthermore, the removal of peel ply is facilitated with the selection of a large fiber diameter, wider warp/weft, and thick peel ply [67,59]. The peel ply manufacturers generally coat the surface of the peel ply using a release agent, such that users can easily remove it from the cured composite. The peeling angle of peel ply removal from composite surface can be set between 135° and 150° to further lighten its removal, as the force required at this angle is the lowest. However, traces of the release agent contain some contaminants (fluorine, nitrogen, or silicon) [33,58,59,57], which significantly degrade bonding properties. Post-treatments, such as light sanding, grit blasting, atmospheric plasma, are performed to remove silicon or fluorine contaminant [15,59].

The second type of peel ply product, tear ply, not only imprints a texture on the composite surface, but also allows a molecular mobility (diffusion) of polymers from the surface of both tear ply and pre-preg, causing the formation of a resin-rich layer. Because of this, tear ply may cause a slight reduction in the bending stiffness of the substrate. Moreover, the tear ply resin is not always compatible with the pre-preg resin [41], increasing the risk of matrix damage upon removal of tear ply from the cured surface [15]. Thus, tear ply is not as popular for treating thermoset composites.

2.2. Solvent cleaning

A solvent is a compound that dissolves other substances, forming a liquid mixture referred to as a solution, without chemically changing them [68]. In the context of surface preparation, solvent cleaning involves a process of removing contaminants (dust, debris, chemicals, release agents) [65] and degreasing [5] the surface of adherends using different types of solvents including isopropanol (IPA) [69], methyl–ethyl–ketone (MEK) [70,24,29], and acetone [7,70]. Solvent cleaning is generally applied to cured composites (thermoset or thermoplastic), plastic, and metals. The underlying mechanism of solvent cleaning involves the selective attraction of the contaminants, and the removal of these contaminants from the surface being cleaned.

The solvent cleaning is performed by simple wiping (using a soft wipe that is fresh, clean, lint-free tissue, or cotton [7]), spraying or using an ultrasonic-assisted technique (bath ultrasonication). When a soft wipe is used, it is ideally used only once to avoid cross-contamination during the wiping process itself [7]. When a soft wipe accidentally introduces particles, such as lint, on the composite surface, blowing dry compressed air is effective to remove these particles. Removing fluorine from the fluoropolymer release film left after the manufacturing of thermoset composites using solvent cleaning may be difficult [24]. Therefore, post-treatment, such as plasma or light sanding, is recommended for this task.

The joint strength or toughness of composite bonded joint cannot be improved simply by solvent cleaning, as this technique is not intended to improve surface roughness or create surface texture [33]. Thus, solvent cleaning is considered as a secondary and finishing treatment that supports other treatments, *e.g.*, grit blasting [71], flame [29], laser [37], and plasma [72].

2.3. Detergent washing

A detergent is a mixture of a surface active agent (surfactant) that is generally used to reduce the surface tension of liquid–liquid, gas–liquid, or solid–liquid. Detergent washing is a cleaning technique that employs a detergent mixed with water to remove contaminants (dirt, oil, grease, silicon, which represent sources of a weak boundary layer [33]) from metallic (aluminum [73,74], steel [75]), composite adherends [33], and bare fibers [76]. Similar to solvent cleaning, detergent washing is not intended to substantially modify the surface morphology or roughness of the adherend, although some detergents are known to moderately erode the surface [77]. The difference between detergent cleaning and solvent cleaning is that the detergent acts by chemically changing the chemistry of the entire surface, while solvent cleaning acts by selectively reducing the surface tension between specific contaminants (grease, metal particles, dirt) and the surface being cleaned. A typical detergent for the removal of contaminants is Alconox (Sigma Aldrich) [73], which can be used for other treatments, *e.g.*, grit blasting. Notably, published literature does not specify a particular detergent for a certain composite type. To speed up the contaminant removal, detergent washing is performed by immersing the composite substrate in the ultrasonic bath [33,77]. This technique has been employed to treat the thermoset composite (carbon/epoxy) and thermoplastic composite (carbon/PEEK, glass/polypropylene) [33]. However, at present, detergent washing is not widespread as a treatment for composites due to two reasons. First, the soluble part of the detergent attaches more efficiently to the adherend surface, replacing and removing the contaminants from the surface. Here, the non-soluble particles eventually become a contaminant to the adherend [78]. Second, although drying is performed, water and detergent residue (particles) may remain on the surface, which may cause swelling in the epoxy-based composites, hence reducing the integrity of materials. Therefore, detergent washing may not be a favored treatment for thermoset-based composites, even though it is only used for cleaning. As an alternative to the detergent, a non-chlorinated solvent (which is environmentally safe) is occasionally employed [78,77].

2.4. Sanding treatment

Sanding is a process of abrading an adherend surface using sandpaper manually by hand or by polishing tools [36]. Sanding is widely-used treatment, as it is cost effective for treating carbon/epoxy [11], glass/epoxy [24], steel [42] and wood; sanding merely requires a sandpaper and relatively short training time for the operator [78]. Furthermore, the modification of surface characteristics (morphology, composition, roughness) and removal of weak boundary layers and contaminants can be rapidly attained by sanding. The strength and/or fracture toughness can be modified by sanding owing to the activation of mechanical interlocking of the adhesive within surface asperities of the substrates [79,33,77].

The most commonly used sandpaper materials for thermoset-based composites are aluminum oxide (Al_2O_3) [24] and silicon carbide

(SiC) [80,36], while the less common material includes nylon (polyamide, PA) [33]. The grains of SiC sandpaper are harder and sharper than those of Al_2O_3, providing a more aggressive abrasion, while Al_2O_3 is more durable, *i.e.*, it has a longer shelf-life compared to SiC. Nevertheless, both are widely used to treat carbon/epoxy or glass/epoxy. A more critical parameter is the grit size (representing sandpaper's roughness). The sandpaper's grit size for treating carbon/epoxy or glass/epoxy ranges between 80 and 800-grit where a lower grit would produce rougher surface [81,34,80,36,82]. Using a grit size below 80-grit severely damages the fibers [81,82], produces heterogeneous peaks and valleys [83], and creates deep valleys that are inaccessible for adhesive infiltration [82]. A short sanding duration of 1–2 min is typically performed to achieve desired roughness and surface deoxidization [70]. A relatively long sanding duration (approx. 5 min), albeit using 320-grit sandpaper, may create a polishing effect (rather than roughening effect). Thus, a low roughness of 0.43 μm was generated in the carbon/epoxy surface [37]. In terms of the sanding direction, random orientation produces better quality than unidirectional sanding (longitudinal, transverse), as random sanding can roughen the surface and clean loose fibers [82]; longitudinal sanding causes isolated fiber bundles, while transverse sanding causes fiber damage. To further improve sanding quality, post-treatment using chemical cleaning (*e.g.*, IPA) is necessary to remove sanding debris [84,37]. It is thus apparent from the above discussion, that the surface characteristics obtained by sanding are highly dependent on the (i) operator skill, (ii) selection of sandpaper materials and grit size, (iii) sanding direction and duration, and (iv) post-sanding treatment [83]. Nonetheless, when carefully carried out, sanding remains one of the simplest treatments for achieving decent roughness, and enhancing mechanical performance of composite bonded joints despite the fact that it may introduce heterogeneous morphology or non-uniform roughness due to its manual nature [37].

2.5. Blasting techniques

Blasting is a process of injecting a highly-pressurized air or nitrogen (N_2) to propel abrasive grains on the adherend surface. Blasting techniques have been employed for treating a relatively large surface area [56] of composites [85,77] and metals [86,73,87]. Users generally must adjust blasting parameters, such as grain materials, grain size (or grit size), gas pressure (around 400 kPa), exposure time, nozzle-to-sample angle, blasting distance, blasting direction, and post-treatment cleaning, to achieve the desired surface morphology, roughness, surface energy, or chemistry [73,77,7,86,88,13]. These parameters must be tuned differently for each of these blasting techniques: grit blasting, cryo-blasting, soda blasting, and wet blasting. For grit blasting (or sand blasting), the commonly selected grain materials are copper [36], Al_2O_3 [85,62,63,89,24,90] and garnet (silicate mineral) [85,88,42]. These materials directly affect the surface energy components of carbon/epoxy substrate. For example, blasting using garnet improves the polar component and reduces the dispersive component more effectively than blasting using Al_2O_3. Garnet is better at removing contaminants, and forming a large number of free-radicals than Al_2O_3 [85], causing the surface to be more nitrogenous (*i.e.*, increasing polar component). In terms of the grit size selected for treating thermoset composites, the commonly-used size is 80–280, which is equivalent to grain sizes below 100 μm. The grain size of Al_2O_3 is 50–70 μm [89,62]. The lower grit size typically yields a rougher morphology in composites; according to the sandpaper principle [85]. To modify the surface energy effectively, the commonly selected grit size is 200–220 [85,88,63].

Although blasting can remove contaminants from the surface and form free radicals (benzoyloxy group that interacts with oxygen, creating oxygen-containing functional groups useful for bonding [85]), it may produce a large amount of residue. A post-treatment, such as solvent cleaning, is used to remove the residue, and maintain the quality of treated surface and expected adhesion [13]. Among these techniques, the lesser utilized blasting techniques for composites are cryo-blasting, soda blasting, and wet blasting. Although they employ a less aggressive material or solution (cryo-blasting uses frozen CO_2 pellets; soda blasting uses non-aggressive grains mixed with sodium bicarbonate; wet blasting uses Al_2O_3 with sodium bicarbonate), they induce severe moisture content in composite materials, causing swelling or debonding. Therefore, their use is not recommended to treat carbon/epoxy or glass/epoxy, which is prone to a harsh infiltration of liquids/solutions during wet blasting.

2.6. Acid and base etchings

Etching has been used to treat thermoset composites for removing contaminants, modifying surface roughness and chemistry, or forming a large amount of pores. The treated composite is usually immersed entirely in a bath containing either an acid or a base solution at specified concentration, temperature, and duration.

The commonly-used acid solution for treating composites includes H_2SO_4 (sulfuric acid), H_2CrO_4 (chromic acid; a mixture of highly-concentrated sulfuric acid and dichromate), HNO_3 (nitric acid), whereas the base solution includes NaOH (sodium hydroxide) [69]. Both acid and base solutions, *e.g.*, H_2SO_4 and NaOH, respectively, have been used to treat thermoset composite (carbon/epoxy). Acid solution has been used to treat thermoplastics (*e.g.*, polyethylene, prior to its bonding with glass/epoxy [18,35]) and thermoplastic composites (*e.g.*, glass/polypropylene for enhancing joint strength [33]). Base solution, such as NaOH, has been used to treat carbon/epoxy although it caused a localized damage to the surface due to its aggressiveness towards the epoxy, causing a reduction of Mode I fracture toughness [69].

Besides the solution type, the concentration level of acidic or base solution significantly modifies the surface chemistry and texture of the adherend. At low concentrations (for example, 27.5 wt% of sulfuric acid, 7.5 wt% of sodium dichromate, and 65 wt% of deionized water [91,74]), etching only modifies the chemical composition of the surface [33], where oxygenated species, such as ester, acids and quinones, are developed [92]. At high concentrations (for example, 98 wt% sulfuric acid [35]), etching yields surface texturing through the removal of surface material and generation of numerous tiny pores that eventually enlarge the overall contact area. These tiny pores can activate the mechanical interlocking between the adhesive and adherend. Nonetheless, albeit effective, careful handling of acid etching is necessary, as it is very toxic (environmentally dangerous), corrosive, and possibly leaves some post-treatment residue that weakens the bonding [18].

2.7. Corona discharge

Corona discharge involves bombarding the target surface using molecules of ionized gas between electrically-charged conductors (*i.e.*, electrodes). The gases commonly used for ionization process include oxygen, argon, ammonia, or sulfur oxide [93]. The gas type generally modifies the chemical elements formed on the treated surface rather than the mechanical performance of the joints [93].

Corona discharge at atmospheric pressure (requiring no vacuum chamber) is applicable for treating thermoset composites (carbon/epoxy) [33,94,34], thermoplastic film [93,18] and thermoplastic composites (carbon/PEEK) [94]. In the treatment of carbon/epoxy or carbon/PEEK, the corona discharge method is advantageous for removing contaminants (*e.g.*, fluorocarbon in carbon/epoxy [33,34], benzene rings in carbon/PEEK [93]), modifying surface morphology (matrix ablation to expose some fibers [94]), modifying surface chemistry (increase in atomic concentration of oxygen in carbon/epoxy; introducing oxidized products of –COO– groups in carbon/PEEK), improving polar component of surface energy [93], wettability (by reducing contact angle) and polarity [34], and enhancing joint strength [33,93,94].

Corona discharge activates the chemical bonding/adsorption mechanism (covalent bonding [94]) between adhesive and adherend of the bonded composites. Although corona discharge involves relatively low cost and is applicable to complex shapes, an open condition (absence of the vacuum chamber) during corona discharge may cause cross-contamination and unstable environmental condition. Issues related to the cross-contamination can be rectified by performing a solvent cleaning [93], and controlling the treatment parameters (discharge duration [94], energy level [93]). Issues related to the unstable condition can be rectified by stabilizing the room temperature and humidity where the corona discharge instrument is located [95]. Moreover, the platform for conducting corona discharge is fairly small, limiting the size of treated specimens.

2.8. Plasma treatment

Plasma treatment aims to introduce a thin plasma layer containing reactive species on the treated surface. These reactive species are usually generated using air [66,96], oxygen [96], nitrogen, fluorine, or inert gases [97]. Similar to corona discharge, plasma treatment is likewise a process that involves electrically charging the plasma-generated particles (electrons, ions, radicals) using two electrodes, and bombarding the charged particles onto the adherend surface. The difference with corona discharge is that the plasma treatment can be performed in either open space (such as in the case of atmospheric pressure plasma treatment) or closed chamber, unlike corona discharge that is usually performed in an open space only [98].

Plasma treatment is used to treat thermoset composites (*e.g.*, glass/epoxy, carbon/epoxy, carbon/polycyanurate) and thermoplastic composites (*e.g.*, glass/PP, carbon/PEEK, carbon/PPS, glass/PPS) [33,99,100,62,65,101,24,80,63,102]. Plasma treatment generally (i) modifies the surface morphology (texture) by introducing an ablation effect that evaporates the matrix phase, (ii) removes contaminants, *e.g.*, oils, greases, release agents [103], and (iii) modifies surface chemistry, *i.e.*, chemical functionalization by substituting the atoms of the surface layer with chemical groups from the plasma [104]. In terms of surface chemistry, plasma treatment reduces carbon content (by 10%–30%), improves oxygen content (by 60%–70%), and nitrogen content (by 0.1–2.2%) [105]. Another chemical modification occurring during plasma treatment is the functionalization between the treated surface and both oxygen and nitrogen that creates moieties (part of molecules, which is larger than functional groups), and changes surface hydrophilicity [105]. All these modifications contribute to the improvement of adhesion between the adhesive and the adherend [103] by the activation of chemical bonding/adsorption and mechanical interlocking.

Nevertheless, the quality of the plasma-treated surface is affected by the plasma condition (atmospheric pressure plasma torch or APPT [105,106], low pressure plasma or cold plasma [25], and low temperature plasma), plasma gas, plasma-to-sample distance [89], exposure time [89,80], raster speed (which can reach 500 mm/s using Plasma-treat AS-400 [66]), gas pressure, flow rates, discharge power, excitation frequency, and material properties of the treated material [33,24,97]. When APPT (within a power range of 96–800 W) is employed, defining the power is important: at low power, APPT can only be used to remove contaminants, whereas at high power, APPT can be used to increase fiber roughness/texture to aid the bonding with the matrix, *e.g.*, carbon-polycarbonate bonding [107]. Cold plasma (power range of 10–200 W; performed within vacuum chamber at 0.5 bar [101,102]) is generally selected to improve wettability and remove contaminants without degrading the existing surface properties (hydrophilicity [27]). The plasma at low temperature is also used for treating a sensitive film by removing the contaminants and activating the surface chemistry, *e.g.*, CNT-dope polyamide-12 interleave film, before being used as an interface/insert in the carbon/epoxy joint [108]. In general, although APPT, cold plasma, or low-temperature plasma can be employed to improve the surface characteristics as well as bonding toughness between adherend and adhesive [101], the chamber dimension is relatively small, sufficient only to store one standard single-lap joint sample [18,101], hence limiting its industrial applicability.

2.9. Flame treatment

Flame treatment utilizes burners that contain an air–gas mixture, which injects a flame through one or more nozzles [97]. The flame can reach a temperature of 900–1000 °C to remove contaminants, modify surface roughness and texture [109], improve hydrophilicity, printability, and paintability [15]. Flame treatment can be used to treat thermoset composites (*e.g.*, carbon/epoxy [29], aramid/epoxy [109]) and thermoplastic materials (*e.g.*, polyolefins such as polypropylene [15] and polyethylene [97]). Parameters affecting the characteristics of the flame treatment include the type of gas compounds, number of passes, treatment duration, scan speed, gas-to-air ratio, flow rates, and the nozzle-to-sample distance. The gases include (i) oxygen with some functional groups [33,18], (ii) liquid petroleum gas (LPG) that contains either silane compounds [29], or propane (C_3H_8) [109]. LPG containing silane compounds enables the deposition of a silicon oxide (SiO_2) layer on the carbon/epoxy surface [29], while LPG containing propane created a thin oxidized layer (< 10 nm thickness) on the polyethylene [97]. Increasing the number of passes was found to reduce the fluorine and carbon contents, and to increase carboxyl (O–C═O) groups [29]. Increasing the flame duration (from 3 to 10 s) was found to modify surface morphology and maximize the surface energy at 44 mJ/m^2 (for a duration of 7 s). Nonetheless, the average surface roughness remains similar for all durations [109]. The scan speed is typically set at 0.04–0.10 s [97]. Reducing the scan speed may induce severe oxidation (burning effect). Optimizing two or more parameters may be necessary to obtain the desired outcome: Brewis et al. [97] maximized the peel strength of polyolefin joints when the scan speed was 0.02 s, while the nozzle-to-sample distance was 10 mm. In terms of the mechanical performance, the shear strength attained by the flame treatment (12 passes) is nevertheless slightly lower than that obtained by conventional sanding process [29]. This is mainly due to the fact that the flame treated adherend has approximately 80% lower surface roughness than that of sanded adherend [110]. Nevertheless, the flame treatment is a promising approach for industrial application owing to its automated process (*e.g.*, movable stage), faster processing rate (*e.g.*, 750 mm/s) and controllable parameters. However, further studies are needed to optimize the flame parameters for applications in thermoset-based composites and other materials.

2.10. Chemical functionalization

Chemical functionalization is a process of replacing atoms on a treated surface (fibers [111,112] or composite [34,113]) with a new functional group (which is also referred to as *fillers surface treatment* [112]). The novel functional group is expected to provide reaction sites for covalent functionalization between adherend and the adhesive. This functionalization enhances polarity, reactivity, wettability, and chemistry of the treated surface, thus enhancing chemical bonding/adsorption and bonding performance.

The steps required for performing this method are simple: (i) pre-treatment of materials, (ii) preparation of a solution containing functional groups or coupling agents, and (iii) application of functionalized solutions to the adherend surface, either by immersion in a bath [34] or by manual spreading using the precision applicator bar [113]. In the pre-treatment process, Jölly et al. [34] employed corona discharge to treat carbon/epoxy before functionalization, while Lee et al. [113] simply used a sandpaper (120-grit) to expose the fibers.

In the application stage, some examples of functionalized solutions for treating carbon/epoxy (T300/970) are GPTMS (organosilane (3-glycidoxypropyl)-trimethoxy silane) [34], TetraThiol (poly-functional

thiol pentaerythritol tetra (3-mercapto propionate)) [34], and a mixture between ethylene glycol (EG) and either graphene oxide (GO) or silane-graphene oxide (sGO). GO aims to improve the mechanical properties of the mixture as it exhibits a high Young's modulus of approximately ~1 TPa. Each solution yields different functionalization outcomes. Here, GPTMS has a functional trialkoxy silane that forms a condensation reaction with hydroxyl groups (–OH) of corona-activated carbon/epoxy surface. TetraThiol has a reaction between the –SH group and oxirane moieties (under the generation of thioethers) that forms a covalent bonding with the corona-activated carbon/epoxy surface [34]. Consequently, GPTMS and TetraThiol enhance the surface energy and wettability of carbon/epoxy surface, thus improving the bonding strength and Mode I fracture toughness of carbon/epoxy joints. In a solution mixture between EG and GO, GO provides hydroxyl, carboxyl, carbonyl (C═O) and epoxide groups that create reaction sites for covalent functionalization with the liquid epoxy (adhesive). In a solution mixture between EG and sGO, sGO provides amine, alkyl, and epoxide groups that create functional layers on the fibers and interact well with liquid epoxy. Notably, sGO was generated by adding a self-assembled monolayer into GO creating functionalized solution, such as GPTMS, APTES ((3-aminopropyl)triethoxysilane), APTMS ((3-aminopropyl)trimethoxysilane), MTES (triethoxymethylsilane) [113]. Here, the reaction sites or the functional layer are characterized by a strong hydrogen bonding between unpaired electrons of the amine group in GO (or sGO) with unpaired electrons of the amide group in liquid epoxy. Therefore, the bonding strength of single-lap joint with GO or sGO treatments can be improved of up to 53% in comparison to the untreated one. Nevertheless, despite the encouraging outcome on the mechanical performance reported by Jölly et al. [34] and Lee et al. [113], several issues remain in the chemical functionalization of thermoset composites, namely the elimination of initial pre-treatment step, controlling the homogeneity and thickness of functionalized layers [112], and ensuring the compatibility between functionalized layers and utilized adhesive [108]. Solving these issues may pave a way for chemical functionalization to be applied as an industrial surface preparation/treatment [114].

2.11. Laser treatment

Laser treatment increases the temperature of the surface, creating a heat affected zone (HAZ) and modifying the chemical elements of the surface [115]. The combustion (oxidation) occurring in the HAZ is dependent on the thermal conductivity of the treated materials [116]. The commonly-used laser type includes the excimer (excited dimer, λ = 248 nm) [117,115,118], UV (ultraviolet, λ = 266 nm [119], 355 nm [120,121]), IR (infrared, λ = 1064 nm) [122,120,123], fiber laser (Nd:YAG, λ = 355 nm [124,114,125]; Yb:KYW or potassium yttrium tungstate, λ = 1024 nm [126,127]; Yb:YAG or ytterbium-doped yttrium aluminum garnet, λ = 1064 nm [128,87,129]), and CO_2 (wavelength λ = 10.6 μm) [56,36,125,130]. Each of these laser types has been used independently to treat thermoset composites for removing contaminants, matrix and fibers from the adherend [119], surface texturing [131], improving surface roughness or changing the morphology, and modifying contact impedance (as a measure of electrical properties) [38].

For example, CO_2 and UV lasers are used to remove silicon contaminants of a release agent found on the carbon/epoxy surface [36,119]. To treat temperature-sensitive materials (neat polymer or polymeric film), the laser illumination of short wavelengths is generally employed, as it exhibits a lower photo-thermal effect on the polymer [39]. The laser technology is feasible for industrial use, as the positioning of the laser beam can be carried out automatically using a guided system. The laser treatment also enables selective surface treatments, rendering the control of the adhesion landscape. As discussed in the following, laser-based surface patterning is an effective strategy for toughening the otherwise brittle CFRP/epoxy interface. Replicating a delicate feature, such as plain woven (peel-ply texture) and crosshatch patterns on carbon/epoxy, is possible using the Nd:YAG fiber laser [132]. Nevertheless, due to numerous parameters involved in the laser system, a proper selection of critical laser parameters is of substantial importance to produce a desired quality of treatment. The critical laser parameters are fluence (energy density, f), power, frequency, number of pulses, distance, and raster speed [124,33]. The magnitude of laser fluence (which is directly related with laser power) used in the removal process of the release agent, matrix, and fibers was proposed by Sun et al. [129]: $f <$ 1.8 J/cm^2 is effective for removing release agent; 1.8 $< f <$ 3.5 J/cm^2 is effective for removing matrix; $f >$ 3.5 J/cm^2 is effective for removing fibers. A high raster speed is important for treating a large composite area in a relatively short time [56]. The laser-to-surface distance is likewise important: Tao et al. [36,37] employed 6 mm distance with a laser fluence of 3.2 J/cm^2 to entirely remove the matrix, leaving bare fibers on the carbon/epoxy surface. Nonetheless, users must optimize the parameters to ascertain the desired outcomes (removal of release agent, matrix, or fibers). For instance, Almuhammadi et al. [83] used the Ytterbium fiber laser, and optimized the laser speed and power for treating carbon/epoxy. A set of speed–power combinations that performs efficiently for an epoxy removal without damaging the fibers was proposed in Ref. [83]. Thus, the laser treatment claims potential for industrial applications due to its versatility for various materials, repeatability, controlled parameters, and automated process.

3. Effects of surface preparation strategies on adhesion mechanisms and phenomenology

3.1. Overview of adhesion mechanisms and phenomenology

Herein, we briefly describe several well-known adhesion mechanisms, namely mechanical interlocking, adsorption/chemical bonding, diffusion and the electrostatic mechanism. These mechanisms are schematically depicted in Fig. 2a–d [133,79,15,134,103,31].

- *Mechanical interlocking* (Fig. 2a) occurs when the adhesive penetrates into the rough or porous adherend surface, enabling mechanical interlocking ("keying") between the adhesive and the adherend [79,135,44].
- *Adsorption/chemical bonding* (Fig. 2b) is the formation of intermolecular bonding caused by forces of attraction between atoms of molecules in the adhesive and those in the adherend [79, 97,135,103,134]. The forces involved are generated by: primary bonds (covalent, ionic, metallic), secondary bonds (van der Waals bonds, hydrogen bonds), and donor–acceptor interactions (*e.g.*, Brønsted acid–base interactions).
- *Diffusion* (Fig. 2c) occurs when the atoms or molecules from two surfaces mutually interdiffuse, such that the initial boundary at the interface is replaced with a new interdiffusional boundary [79] or interphase [136]. This process incorporates an entanglement of long-chain molecules [31]. The molecules from both surfaces must be mobile, compatible, and miscible [44] to yield a strong adhesion [44,103].
- *Electrostatic adhesion* (Fig. 2d) suggests that there is a transfer of electrons from one surface to another when the two are in contact. Consequently, the double-layer system (positively- and negatively-charged layers) is formed, which introduces forces of attraction [97].

3.2. Adhesion mechanisms activated by surface preparations

Table 1 lists possible effects of surface preparation/treatment on the activation of adhesion mechanisms and removal of weak boundary layer in secondary bonding. Here, *mechanical interlocking* can be directly activated by sanding, blasting techniques, peel ply, etching, plasma, flame, and laser due to the enhancement of surface indicators,

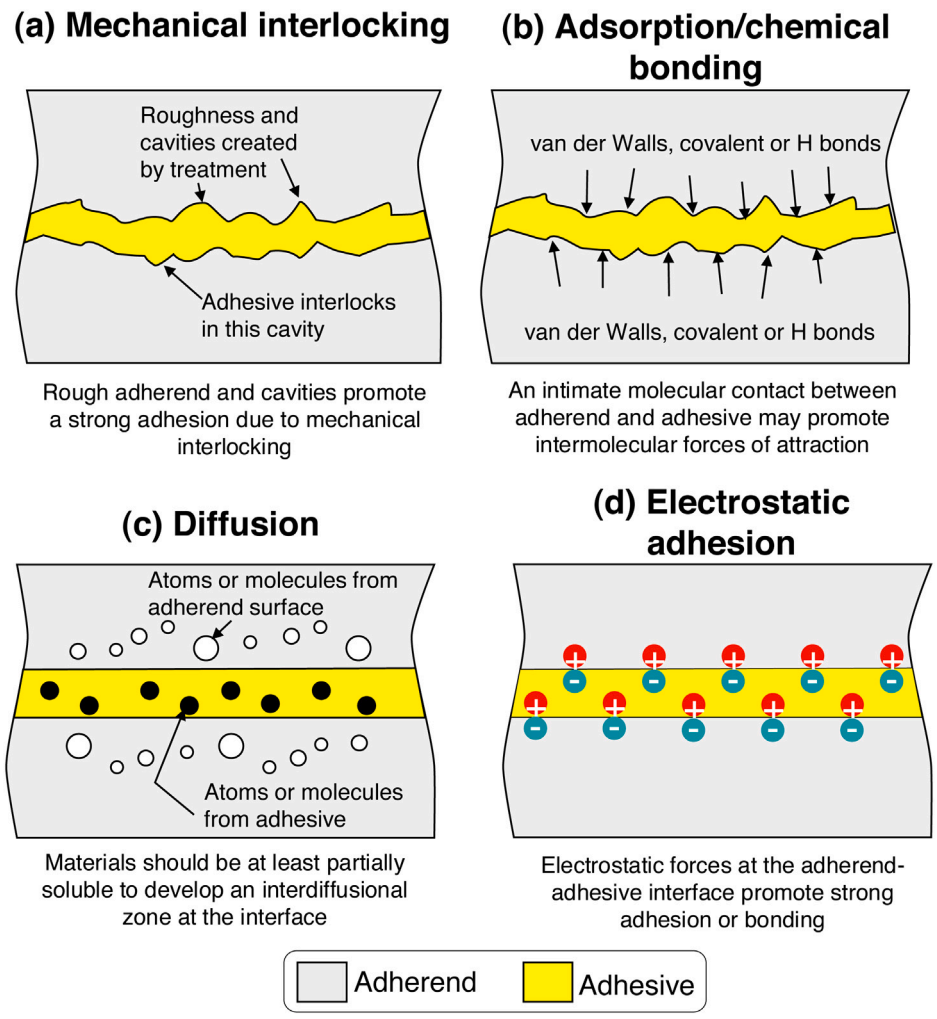

Fig. 2. Adhesion mechanisms and phenomenology: (a) mechanical interlocking, (b) adsorption/chemical bonding, (c) diffusion, (d) electrostatic adhesion.

Table 1
The role of surface preparation/treatment on the activation of adhesion mechanisms (see Fig. 2 as a reference for these mechanisms) and removal of weak boundary layer in secondary bonding.

Surface preparation	Role of surface preparation	Ref.
Sanding	Mechanical interlocking, adsorption/chemical bonding	[34,82]
Blasting technique	Mechanical interlocking, adsorption/chemical bonding	[63,62]
Peel ply	Mechanical interlocking, adsorption/chemical bonding	[63,55]
Tear ply	Diffusion	[63,55]
Solvent cleaning	Removal of weak boundary layer	[33]
Detergent washing	Removal of weak boundary layer	[33]
Etching	Mechanical interlocking, removal of weak boundary layer	[35]
Chemical functionalization	Adsorption/chemical bonding	[34,113]
Corona discharge	Adsorption/chemical bonding	[93]
Plasma treatment	Mechanical interlocking, adsorption/chemical bonding	[63]
Flame treatment	Mechanical interlocking, adsorption/chemical bonding	[29]
Laser treatment	Mechanical interlocking, adsorption/chemical bonding	[36]

such as morphological changes (e.g., "ink-bottle" feature, possibly achieved by sanding or blasting techniques, that strengthens the interlocking [79]), topography metrics (roughness, contact angle) [63], and modification of surface energy and surface composition (removal of a weak boundary layer or contaminated surface) [79,77,44]. *Adsorption/chemical bonding* may be activated by blasting techniques, peel ply, chemical functionalization, corona discharge, plasma, flame, and laser, as these treatments generally increase the surface energy and promote the formation of covalent or hydrogen bonding (particularly, plasma treatment). The *diffusion process* is generally activated by the tear ply method, where the resin surface of the pre-preg is mixed with the one from the tear ply, forming a new resin layer [58]. All these mechanisms build a synergy that contributes to the improvement of mechanical indicators generally quantified by joint strength and toughness. The *electrostatic adhesion* generally does not occur in non-conductive materials, such as thermoset composites. Moreover, the effect of surface preparation methods on the activation of electrostatic mechanism is not reported on the literature. Thus, whether surface preparation can affect the electrostatic adhesion is not conclusive to date.

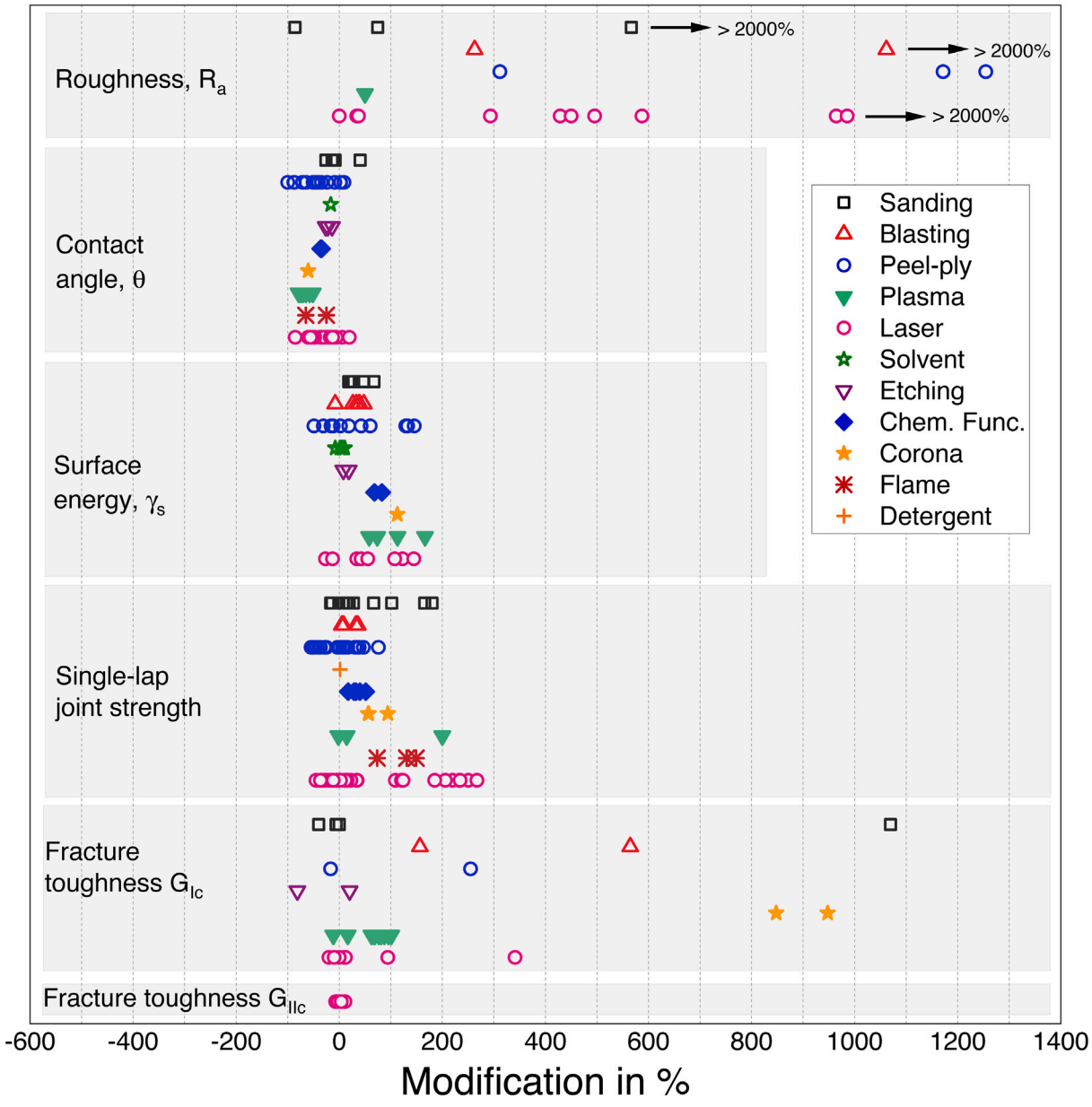

Fig. 3. Modification of surface (roughness, contact angle, surface energy) and mechanical indicators (single-lap joint strength, Mode I and Mode II fracture toughness) of thermoset composites by various surface treatments. The modification in % is calculated based on the values of untreated specimens.

4. Effects of surface preparation strategies on surface and mechanical indicators

The modification of surface and mechanical indicators due to the surface preparation in composites is a complex process. Optimizing surface preparation is necessary to evaluate how processing parameters influence the bonding process, whereas performing a full-scale test on structures with adhesively bonded joints might be prohibitive due to both cost and time constraints. Therefore, relatively rapid techniques to evaluate the effect of surface preparations on surface and mechanical indicators must be introduced. In the subsequent two sections, we review the most common metrics related to the (1) surface and (2) mechanical indicators that can be used to evaluate the influence of a specific surface preparation. We further provide a summary of modifications affected by a specific treatment in terms of surface indicators (roughness, R_a; contact angle, θ; surface energy, γ_s) and mechanical indicators (single-lap joint strength; fracture toughness in Mode I, G_{Ic}; fracture toughness in Mode II, G_{IIc}). As shown in Fig. 3, the level of modification is given in percentages, and it is compared with the indicators of untreated surface.

4.1. Surface indicators

4.1.1. Morphology

Surface treatment generally modifies the topology and texture of the thermoset composite surface [114,123], although some treatments only remove contaminants, barely modifying the surface morphology. The observation of surface morphology is generally performed by the optical microscope [132,114], scanning electron microscope (SEM) [37], or atomic force microscope (AFM) [69]. These morphology observations are mostly qualitative, and serve as the first step to ascertain the existence of morphological changes.

SEM images of surface morphology of composites after treatment are shown in Fig. 4. It is evident that peel ply, sanding, blasting, corona discharge, flame, and laser treatments induce morphological changes to the composite surface. The morphology of carbon/epoxy

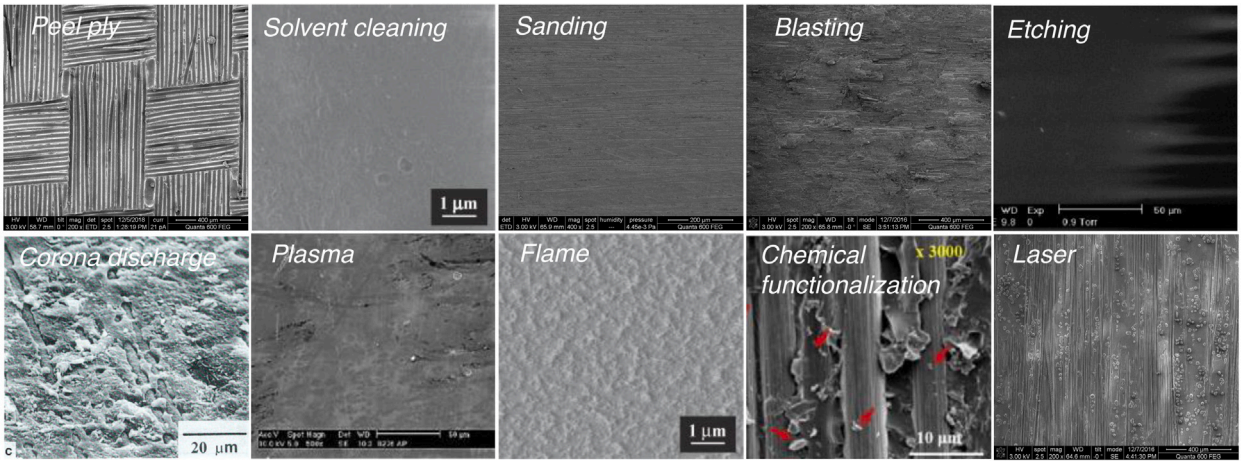

Fig. 4. SEM images of surface morphology of composites after treatments: peel ply [36], solvent cleaning [29], sanding [37], blasting [36], etching [69], corona discharge [94], plasma [24], flame [29], chemical functionalization (arrows indicate location of graphene/oxide) [113], laser [36].

after the peel ply treatment shown in Fig. 4 conforms with the plain woven peel ply pattern. Sanding using SiC sandpaper modifies the original texture by the removal of epoxy layer and some surface fibers, imparting a roughening effect on the surface [37]. However, a long duration of sanding (> 5 min) using 60–80 grit could damage the fibers instead of polishing or roughening the surface [24,36]. Similar to sanding, blasting could generally roughen the surface [24]; however, copper grains are found to induce severe damage to the matrix and fibers [36]. Corona discharge, plasma, flame, and laser treatments are effectively controllable to produce a desired outcome. Corona discharge can be used for light removal of the matrix, avoiding the risk of fiber damage. Although plasma is generally used to remove the thin layer of matrix, smoothen the surface, and remove the contaminants [66], plasma treatment with a long exposure time may cause discoloration and matrix damage as the surface temperature could reach 164 °C [89]. A relatively rougher texture in comparison to that by plasma can be obtained by flame treatment [29]. Laser treatment (using CO_2) produces a rough surface in the carbon/epoxy due to the contour of the sub-surface fibers upon the removal of a thin epoxy layer. However, a high laser fluence (f > 3.2 J/cm^2) can fully remove the epoxy, inevitably breaking some carbon fibers [37,53].

In contrast to the above treatments, solvent cleaning, detergent washing, acid etching or chemical functionalization do not impart a significant change to the surface morphology of the composite. The surface morphology of the composite treated with solvent cleaning and detergent washing is similar to the pristine one, since these treatments are generally used for cleaning or removing contaminants only. Likewise, as depicted in Fig. 4, nitric acid etching did not induce a significant change to the morphology. In contrast, base etching using sodium hydroxide may induce local matrix damage on the composite [69]. Chemical functionalization does not modify surface morphology, except by a dispersion of particles, *e.g.*, graphene oxide, that may exfoliate the fibers and the matrix. Therefore, chemical functionalization is typically performed after the treatments produce morphological changes (*e.g.*, sanding) to improve joint strength [113].

4.1.2. Topography metrics

The direct influence of treatments on a surface of adherend/substrate is generally quantified using topography metrics, *i.e.*, surface roughness. The roughness represents a series of normal deviations, characterized by peaks and valleys of varying space, height, and depth of a solid surface. A rougher surface is generally desirable, as it provides a stronger intrinsic adhesion associated with the increase in surface energy [86], and an effective contact area between adhesive and adherend that activates the mechanical interlocking mechanism [79], redistribution of stresses in the adhesive, and change of failure mechanism that causes a higher energy dissipation before final failure [86]. Increasing the surface roughness is expected to improve the strength and toughness of adhesively-bonded joint [137].

The surface roughness (R_a) can be directly measured using a profilometer [86], where a soft stylus would probe numerous points of peaks and valleys along pre-defined axis (x- or y-axis) and for a certain length on the surface [138,36]. Some examples of the profilometer include Mitutoyo SJ-301 [62], Veeco Dektak 150 [36]. Fig. 5a shows the surface of grit-blasted carbon/epoxy as observed by SEM, and roughness measurement in x- and y-directions. For a very small area (10 × 10 micron), atomic force microscopy (AFM) can be used to measure the surface roughness [98]. A topography mapping, which is exemplified in Fig. 5b [37] where an 3D optical surface profiler is employed, provides a roughness measurement in two-dimension. To enhance the measurement accuracy, the surface must be coated with a thin Au layer of around 25 nm.

Here, we compiled the values of R_a (regardless of the measurement axis), as most published studies reporting the roughness of carbon/epoxy or glass/epoxy after treatment usually provide R_a values. The variations of R_a in carbon/epoxy and glass/epoxy treated with various techniques is given in Table 2. The data reported in the literature mostly deals with following treatments: sanding, grit blasting, peel ply, plasma, and laser (CO_2, fiber, excimer). Furthermore, we found that carbon/epoxy receives a great interest in comparison to glass/epoxy (the data available for the latter is limited to peel ply and laser excimer treatments). Table 2 shows that most surface treatments increase the surface roughness of carbon/epoxy and glass/epoxy between 34% and up to more than 2000%. The reduction of roughness by 86% was reported by Tao et al. [37] when SiC sanding was employed in the treatment of carbon/epoxy. This is due to the fact that the reference value of untreated surface had a roughness equal to 3.06 μm, while the roughness of the sanded surface was 0.43 μm (similar to the value reported by Liu [139], *i.e.*, 0.475 μm). The reduction was also possibly caused by a relatively long sanding duration of 5 min using a rotating machine at 300 rpm, resulting in a considerably flat surface. Grit blasting (either using copper or alumina) increases the surface roughness of carbon/epoxy by more than 10×. Peel ply typically increases roughness by a factor of 3–25× compared to the untreated surface [54,37,62]. The CO_2 laser and atmospheric plasma produced a small increase in the roughness (30%–50%) of the carbon/epoxy. In the fiber laser treatment, increasing fluence (or power) and pulse number could generally increase the surface roughness. Increasing the laser fluence from 0.15 to 0.50 J/cm^2 generally improves the roughness of the glass/epoxy's surface by 30× [118]. Increasing the number of

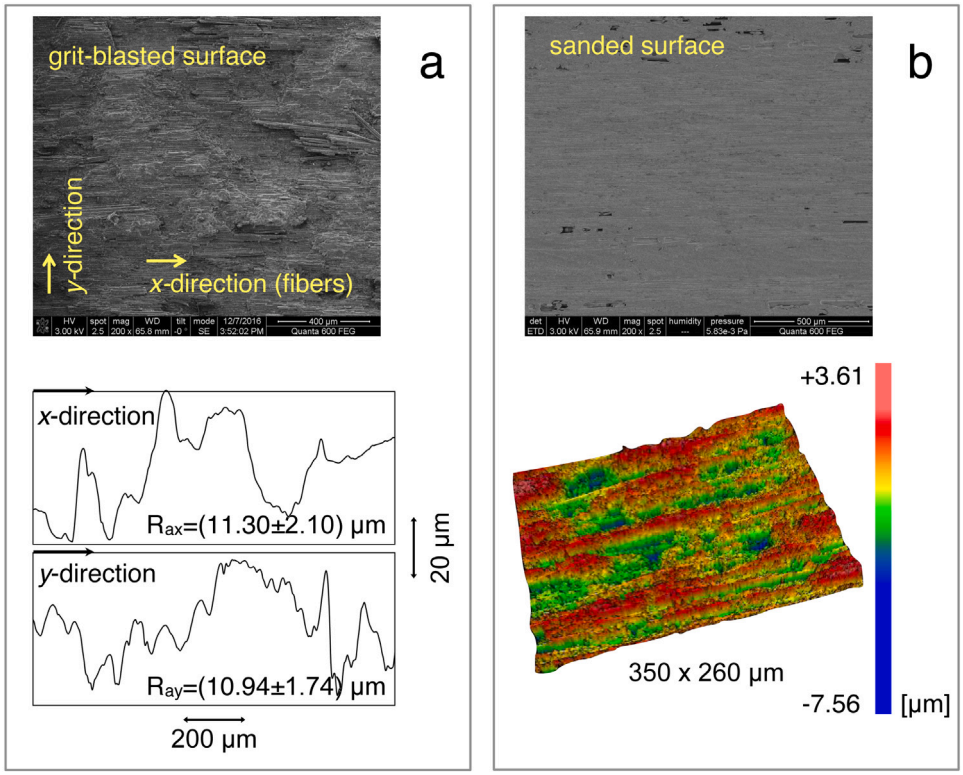

Fig. 5. (a) Roughness measurement in x- and *y*-axis of grit-blasted carbon/epoxy surface using profilometer [36], (b) topography map of sanded surface of carbon/epoxy obtained from 3D optical profiler [37].

Table 2
Reported effects of surface treatment on surface roughness R_a of carbon/epoxy and glass/epoxy. The variation in percentage (var. %) is calculated based on the values of untreated specimens.

Treatment	Adherend	R_a (var. %)	Ref.
Sanding (SiC, 150-grit)	C/E	+2567	[34]
Sanding (SiC, 320-grit)	C/E	−86	[37]
Sanding (SiC, 320-grit)	C/E	+75	[139]
Grit blasting (copper)	C/E	+263	[36]
Grit blasting (Al_2O_3, 220-grit)	C/E	+1062	[62]
Peel ply (PA, plain woven)	C/E	+312	[37]
Peel ply (polyester, plain woven)	C/E	+2488	[62]
Peel ply (-)	C/E	+1254	[61]
Peel ply (-)	G/E	+1172	[61]
Plasma	C/E	+50	[62]
Laser (CO_2, f = 1.2 J/cm^2)	C/E	+34	[37]
Laser (CO_2, f = 3.6 J/cm^2)	C/E	+37	[37]
Laser (fiber, f = 1.0 J/cm^2)	C/E	+429	[129]
Laser (fiber, f = 3.5 J/cm^2)	C/E	+964	[129]
Laser (fiber, f = 7.0 J/cm^2)	C/E	+986	[129]
Laser (IPG, P = 80 W)	C/E	+293	[139]
Laser (IPG, P = 120 W)	C/E	+588	[139]
Laser (IPG, P = 180 W)	C/E	+496	[139]
Laser (excimer, f = 0.15 J/cm^2, 40 pulses)	G/E	0	[118]
Laser (excimer, f = 0.15 J/cm^2, 50 pulses)	G/E	+450	[118]
Laser (excimer, f = 0.15 J/cm^2, 400 pulses)	G/E	+2083	[118]
Laser (excimer, f = 0.50 J/cm^2, 500 pulses)	G/E	+2767	[118]

Note: f and P denote fluence (laser energy density) and power, respectively, used in laser treatment; C/E denotes carbon/epoxy; G/E denotes glass/epoxy; PA denotes polyamide.

laser pulses (excimer with f = 0.15 J/cm^2) from 40 to 50 pulses could increase the roughness from 0.6 to 3.3 μm [118]. Higher laser fluences in the CO_2 laser treatment increased the roughness only by 34%–37%.

In summary, the reviewed surface treatments mostly increase the roughness of around 600% (although, in a few cases, the roughness modification can exceed 2000%), which is achieved by sanding (using SiC sandpaper), peel ply (polyester), and laser excimer.

4.1.3. Contact angle and surface energy

Contact angle θ is an angle made a droplet of liquid and a solid surface (see Fig. 6a). Here, $\theta = 0°$ represents a perfect wetting, $\theta < 90°$ represents hydrophilic surface (i.e., good wettability; see Fig. 6b), and $\theta > 90°$ represents hydrophobic surface (i.e., poor wettability; see Fig. 6c). The contact angle can be measured using the sessile drop technique (among others), where a small amount of a liquid (water, glycerol, formamide, diiodomethane, or ethylene glycol [54]) is dropped on a solid surface, while an optical microscope is used to

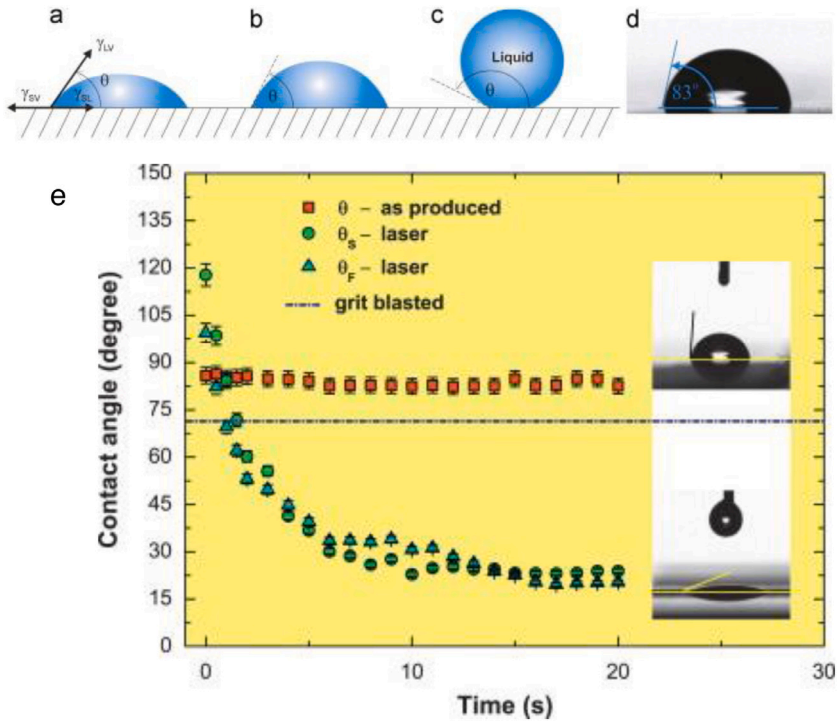

Fig. 6. (a) Equilibrium state of a droplet on a solid surface, (b) contact angle of hydrophilic surface showing that good wetting occurs when $\theta < 90°$, (c) contact angle of hydrophobic surface showing that poor wetting occurs when $\theta > 90°$, (d) an example of glycerol droplet on a solid surface as observed during the sessile technique, (e) an example of contact angle measurement of non-treated (as produced), grit blasted and laser-treated samples [87].

take the side-view image of a droplet for subsequently estimating the magnitude of θ. Fig. 6d shows an example of glycerol droplet dropped on a surface [87]. Surface treatment generally aims to reduce θ. Fig. 6e shows the influence of laser on contact angle of a material, where θ is significantly reduced due to laser-based surface preparation. It should be noted that θ is generally dependent on surface roughness [140,141,87,142]. Wenzel [140] proposed a parameter r, which is the ratio between actual surface of the rough area A_a and the projected surface of the rough area A_p. Wenzel theory is generally used to obtain the contact angle of a rough surface θ_f from the information about the contact angle of a smooth surface θ_s as follows

$$\cos\theta_f = \frac{A_a}{A_p}\cos\theta_s = r\cos\theta_s \tag{1}$$

A summary of contact angle variations of thermoset composites after surface treatment is given in Table 3. Here, the peel ply yields the highest reduction in the contact angle, achieving 100% reduction. A more consistent outcome is produced by polyamide peel ply rather than polyester peel ply [54]. Etching likewise improves wettability, despite its dependence on the etching duration, *i.e.*, the longer etching (of 120 min) improves wettability by 26% compared to shorter etching (of 1 min) [35]. Plasma treatment also reduces the contact angle of up to 77%, although this is dependent on the exposure time and composite types [80].

Nevertheless, relying only on the contact angle alone for measuring wettability is not recommended for estimating the bond quality in adhesively-bonded joints [64,80]. It is necessary to proceed with the calculation of the surface energy γ_s using contact angle measurement results [64]. The relationship between the surface energy of solid–vapor γ_{sv} and surface energy of solid–liquid γ_{lv} is shown in Fig. 6a. This relationship can be calculated using Young's equation and Owens–Wendt theory:

$$\frac{\gamma_{lv}(\cos\theta+1)}{2\sqrt{\gamma_{lv}^d}} = \frac{\sqrt{\gamma_{lv}^p}}{\sqrt{\gamma_{lv}^d}}\sqrt{\gamma_{sv}^p} + \sqrt{\gamma_{sv}^d}, \tag{2}$$

where the superscripts d and p represent dispersive and polar components of the surface energy, respectively, which satisfy the following conditions:

$$\gamma_{lv} = \gamma_{lv}^d + \gamma_{lv}^p, \tag{3}$$

$$\gamma_{sv} = \gamma_{sv}^d + \gamma_{sv}^p. \tag{4}$$

Evidently, calculating the surface energy requires the measurement of dispersive and polar components, which can be achieved by using sequentially different liquids with a priori known dispersive and polar components (water, glycerol, formamide, diiodomethane, and EG [54]).

Table 4 shows the modification of the surface energy resulting from various treatments. Sanding improves the surface energy of the carbon/epoxy by 10%–50% due to roughness that is imparted by different grits. Grit blasting using alumina produces a comparable surface energy with peel ply. Blasting produces a balanced ratio of dispersive and polar components [63]. Peel ply improves surface energy in epoxy-based composite by more than 50% [61]. It overwhelmingly affects mostly the polar component (nitrogenous species; useful for increasing molecular forces and adhesion between polymers), rather than the dispersive component (carbonated species) [58,54]. However, peel ply made of polyamide introduces more polar groups, while that made of polyester introduces non-polar groups [54]. Although polyester introduces a larger amount of non-polar groups to the surface, the contribution of roughness to the adhesion enhancement (introduced by the peel ply pattern in both polyester) is more dominant than the contribution of molecular forces generated by the polarity level [54]. Further enhancement of surface energy can be attained by combining different treatments. For example, combining peel ply and atmospheric plasma treatments in treating carbon/epoxy (IM7/8552) provides a significant improvement of the total surface energy in comparison to using only peel ply or PTFE [66].

In summary, we found that most treatments (sanding, peel ply, solvent, etching, chemical functionalization, corona, plasma, flame, and

Table 3
Reported effects of surface treatment on contact angle θ of carbon/epoxy and glass/epoxy. The variation in percentage (var. %) is calculated based on the values of untreated specimens.

Treatment	Adherend	Liquid	θ (var. %)	Ref.
Sanding (SiC, 120-grit)	C/E (M21)	W	−8	[80]
Sanding (SiC, 120-grit)	C/E (DT120)	W	+41	[80]
Sanding (SiC, 280-grit)	C/E	–	−14	[98]
Sanding (SiC, 320-grit)	C/E	W	−9	[139]
Sanding (SiC, 320-grit)	C/E	G	−14	[139]
Sanding (Al_2O_3, 120-grit)	C/E	W	−26	[69]
Peel ply (polyamide)	C/E	W	−41	[54]
Peel ply (polyamide)	C/E	GL	−49	[54]
Peel ply (polyamide)	C/E	FD	−48	[54]
Peel ply (polyamide)	C/E	MI	−71	[54]
Peel ply (polyamide)	C/E	EG	−71	[54]
Peel ply (polyamide)	G/E	W	−51	[54]
Peel ply (polyamide)	G/E	GL	−42	[54]
Peel ply (polyamide)	G/E	FD	−46	[54]
Peel ply (polyamide)	G/E	MI	−71	[54]
Peel ply (polyamide)	G/E	EG	−64	[54]
Peel ply (polyester)	C/E	W	−24	[69]
Peel ply (polyester)	C/E	W	+3	[54]
Peel ply (polyester)	C/E	GL	−44	[54]
Peel ply (polyester)	C/E	FD	−48	[54]
Peel ply (polyester)	C/E	MI	−100	[54]
Peel ply (polyester)	C/E	EG	−87	[54]
Peel ply (polyester)	G/E	W	+2	[54]
Peel ply (polyester)	G/E	GL	−35	[54]
Peel ply (polyester)	G/E	FD	−48	[54]
Peel ply (polyester)	G/E	MI	−100	[54]
Peel ply (polyester)	G/E	EG	−88	[54]
Peel ply (-)	C/E	W	−9	[122]
Peel ply (-)	C/E	GL	+9	[122]
Solvent cleaning (IPA)	C/E	W	−16	[69]
Chem. func. (Trialkoxy silanes)	C/E	W	−34	[34]
Chem. func. (Thiols)	C/E	W	−36	[34]
Etching (acid, HNO_3)	C/E	W	−14	[69]
Etching (acid, H_2SO_4)	G/E	EP	−26	[35]
Etching (base, NaOH)	C/E	W	−22	[69]
Corona (-)	C/E	W	+36	[34]
Plasma (t = 15 s)	C/E	W	−51	[80]
Plasma (t = 30 s)	C/E	W	−70	[80]
Plasma (t = 45 s)	C/E	W	−77	[80]
Plasma (t = 60 s)	C/E	W	−74	[80]
Plasma (t = 75 s)	C/E	W	−65	[80]
Plasma (pass = 1)	C/E	–	−58	[98]
Plasma (pass = 3)	C/E	–	−71	[98]
Plasma (pass = 6)	C/E	–	−76	[98]
Plasma (pass = 12)	C/E	–	−78	[98]
Plasma (pass = 24)	C/E	–	−79	[98]
Plasma (pass = 48)	C/E	–	−79	[98]
Laser (fiber, f = 3.5 J/cm^2)	C/E	W	−26	[129]
Laser (fiber, f = 3.5 J/cm^2)	C/E	MI	−6	[129]
Laser (fiber, f = 3.5 J/cm^2)	C/E	EG	−35	[129]
Laser (IR, IPG:YLP)	C/E	W	+6	[122]
Laser (IR, IPG:YLP)	C/E	G	+20	[122]
Laser (IPG, P = 80 W)	C/E	W	−24	[139]
Laser (IPG, P = 80 W)	C/E	GL	−21	[139]
Laser (IPG, P = 120 W)	C/E	W	−38	[139]
Laser (IPG, P = 120 W)	C/E	GL	−85	[139]
Laser (IPG, P = 180 W)	C/E	W	−30	[139]
Laser (IPG, P = 180 W)	C/E	GL	−57	[139]
Laser (excimer, f = 0.15 J/cm^2, 1 pulse)	C/E	W	−10	[118]
Laser (excimer, f = 0.15 J/cm^2, 1 pulse)	C/E	GL	−17	[118]
Laser (excimer, f = 0.15 J/cm^2, 1 pulse)	C/E	FD	−48	[118]
Laser (excimer, f = 0.15 J/cm^2, 1 pulse)	C/E	MI	−60	[118]
Laser (excimer, f = 0.15 J/cm^2, 1 pulse)	C/E	EG	−52	[118]
Laser (excimer, f = 0.15 J/cm^2, 10 pulses)	C/E	W	−6	[118]
Laser (excimer, f = 0.15 J/cm^2, 10 pulses)	C/E	GL	−13	[118]
Laser (excimer, f = 0.15 J/cm^2, 10 pulses)	C/E	FD	−55	[118]
Laser (excimer, f = 0.15 J/cm^2, 10 pulses)	C/E	MI	−51	[118]
Laser (excimer, f = 0.15 J/cm^2, 10 pulses)	C/E	EG	−56	[118]

Note: f, fluence; C/E, carbon/epoxy; G/E, glass/epoxy; W, water; GL, glycerol; FD, formamide; MI, diiodomethane; EG, ethylene-glycol; EP, epon-828 liquid epoxy.

laser) reduce the contact angle up to 100% (Fig. 3), thus improving the surface energy of composites prior to bonding. Attention must be paid to the application of the (i) sanding process for the possibility of causing non-uniform roughness, (ii) peel ply, blasting, solvent or laser (excimer, IR) that possibly reduce the surface energy. Finally,

Table 4
Reported effects of surface treatment on surface energy γ_s of carbon/epoxy and glass/epoxy. The variation in percentage (var. %) is calculated based on the values of untreated specimens.

Treatment	Adherend	γ_s (var. %)	Ref.
Sanding (SiC, 150-grit)	C/E	+48	[34]
Sanding (SiC, 320-grit)	C/E	+23	[36]
Sanding (SiC, 320-grit)	C/E	+28	[139]
Sanding (Al_2O_3, T-9 grit)	C/E	+67	[24]
Sanding (Al_2O_3, T-9 grit)	G/E	+18	[24]
Sanding (Al_2O_3, 120-grit)	C/E	+26	[69]
Grit blasting (garnet, 80-grit)	G/E	+33	[85]
Grit blasting (garnet, 220-grit)	G/E	+40	[85]
Grit blasting (Al_2O_3, 220-grit)	C/E	−8	[62]
Grit blasting (Al_2O_3, 220-grit)	G/E	+38	[85]
Grit blasting (Al_2O_3, 240-grit)	C/E	+48	[24]
Grit blasting (Al_2O_3, 240-grit)	G/E	+26	[24]
Peel ply (polyamide, plain)	C/E	+145	[59]
Peel ply (polyamide, plain)	C/E	−49	[59]
Peel ply (polyamide, plain)	C/E	+133	[59]
Peel ply (polyamide, twill)	C/E	+129	[59]
Peel ply (polyester)	C/E	−12	[62]
Peel ply (polyester)	C/E	+18	[69]
Peel ply (glass)	C/E	−31	[59]
Peel ply (glass)	C/E	+2	[66]
Peel ply (-)	C/E	+43	[54]
Peel ply (-)	C/E	−16	[122]
Peel ply (-)	G/E	+60	[54]
Solvent cleaning (IPA)	C/E	+11	[69]
Solvent cleaning (IPA)	C/E	+5	[24]
Solvent cleaning (IPA)	G/E	+1	[24]
Solvent cleaning (MEK)	C/E	+7	[24]
Solvent cleaning (MEK)	G/E	−8	[24]
Chem. func.	C/E	+68	[34]
Chem. func.	C/E	+83	[34]
Etching (acid, HNO_3)	C/E	+8	[69]
Etching (base, NaOH)	C/E	+18	[69]
Corona	C/E	+113	[34]
Plasma atmospheric	C/E	+58	[62]
Plasma atmospheric	C/E	+113	[24]
Plasma atmospheric	C/E	+166	[66]
Plasma atmospheric	G/E	+74	[24]
Flame	C/E	+155	[110]
Laser (CO_2, f = 1.2 J/cm^2)	C/E	+123	[36]
Laser (fiber, f = 3.5 J/cm^2)	C/E	+34	[129]
Laser (IR, IPG:YLP)	C/E	−27	[122]
Laser (IPG, P = 80 W)	C/E	+42	[139]
Laser (IPG, P = 120 W)	C/E	+145	[139]
Laser (IPG, P = 180 W)	C/E	+108	[139]
Laser (excimer, f = 0.5 J/cm^2)	C/E	−13	[117]
Laser (excimer, f = 1.0 J/cm^2)	C/E	+55	[117]

Note: f, fluence; P, power; C/E, carbon/epoxy; G/E, glass/epoxy.

of all aforementioned treatments, the most effective with regard to improvement of the surface energy is the plasma treatment.

4.1.4. Surface composition

The surface treatment modifies the surface chemistry of a treated surface. Understanding the presence of certain chemical elements (carbon, oxygen, nitrogen, sulfur, silicon, and fluorine [117,143]) and functional groups (silicon dioxide SiO_2 [29], alkoxy C–O, carbonyl, carboxyl, and others [37]) after the surface treatment is essential for improving adhesion quality between the adhesive and adherend [97]. The quantification of these chemical elements and functional groups is carried out using XPS (X-ray Photoelectron Spectroscopy; to determine elemental concentration) [143], FTIR (Fourier-Transform Infrared Spectroscopy; to provide high-spectral-resolution data over a wide spectral range of absorption or emission), Auger electron spectroscopy, and time-of-flight secondary ion mass spectrometry (ToF-SIMS) [97].

Table 5 summarizes the chemical elements and functional groups reported in various studies. Treatments may introduce unwanted or detrimental chemical elements, *e.g.*, release agent or coating for the mold in the manufacture of composites [29]. The unwanted chemical elements, namely silicon (Si), sulfur (S), fluorine (F), could potentially produce a weak boundary layer. The desired functional groups useful for the adhesion are hydroxyl, carboxyl, oxygen aliphatic, and aromatic groups.

The peel ply treatment typically introduces silicon [37] and fluorine [24] to the composite adherend. These contaminants are generated by the release agent coated on the original peel ply prior to implementation. It is noteworthy that fluorine cannot be removed by the MEK solvent wipe [29]. Instead, sanding or blasting can be used to remove the silicon or fluorine. However, the original peel ply texture might be slightly altered [24], and the generation of debris is inevitable, thus requiring cleaning. The flame treatment (ITRO) with 12 passes can reduce the fluorine content from carbon/epoxy surface by 75% [29]. Furthermore, the flame treatment can form a SiO_2 layer that can connect with hydroxyl groups, and increase the concentration of carbonyl and carboxyl groups, both of which results in the enhanced surface energy to yield a strong adhesion [29]. Chemical functionalization using GO and sGO improves surface chemistry by providing reaction sites for covalent functionalization (abundance of functional groups such as hydroxyl, carboxyl, carbonyl, epoxide) [113]. The plasma treatment also introduces a higher amount of oxidized functional groups that reduce the contact angle and improve surface wettability [80].

In summary, as shown in Table 5, most treatments introduce chemical elements or groups that are useful for improving adhesion, while

Table 5
Useful and unwanted chemical groups during treatment of composites.

Criterion	Elements or chemical groups	Treatment	Ref.
Useful	C, O, N	Sanding	[34,139]
	C, O, C–O, C=O O–C=O, C–N, NC=O	Blasting	[36]
	O, N, C–O, C=O/C–OH C–C/C–H, C_6H_5, C_7H_7	Peel ply	[58,59]
	C–H, C=O, C–O, O–C=O	Solvent	[29]
	C, O	Chemical func.	[34]
	C, O, N	Corona	[34]
	C, O, N, C–C, C–OH, C–COOH C=O, C–O, O–C=O	Plasma	[65,108]
	C, O, C–H, C=O, C–O, O–C=O	Flame	[29]
	C, O, N, C–OH, C=O, O–C=O, C–C C–O, O-C=O, COOH, CO_3^2	Laser	[36,123,107,139]
Unwanted	Si	Blasting	[36]
	Si, F, S, CF_2	Peel ply	[58,59]
	Si, S	Chemical func.	[34]
	Si, F	Plasma	[65,108]
	Si, F	Flame	[29]
	Si, S	Laser	[36,123,107,139]

some treatments evidently impart some unwanted chemical elements/groups, such as silica, fluorine. Peel ply, for instance, introduces more unwanted chemicals to the adherend surface than other treatments, e.g., silica, fluorine, and difluorocarbene (CF_2). Indeed, the unwanted chemical generated by other treatments than peel ply can be the residual surface contamination, not necessarily generated by the treatment itself. Nonetheless, these unwanted chemicals should be avoided as they are detrimental to the bonding integrity between adherends in secondary bonded joints.

4.2. Mechanical indicators

4.2.1. Strength of composite joints

The surface treatment generally affects the strength of composite bonded joints, which can be evaluated by performing the lap joint test (single-lap joint, ASTM D5868 [144]) or peel tests (fixed arm, T-peel of ASTM D1876 [145], floating roller test of ASTM D3167 [146,147], climbing drum of ASTM D1781 [148], mandrel peel [149]). The single-lap joint (SLJ) test, in particular, has received widespread interest because of its simple preparation, straightforward testing method (unidirectional tensile test), and direct outcome. The SLJ test directly generates the maximum strength $\tau_{max} = P_{max}/(LB)$, where P_{max} is the attained maximum load, L is the overlap length, and B is the specimen width [26]. Therefore, several theoretical formulae for predicting the joint strength based on the stresses (shear and peel) in the adhesive bondline have been developed in Ref. [79,150–153]; these formulae are beyond the scope of this review paper.

The SLJ strength data in relation with the surface treatment is tabulated in Table 6. Sanding and blasting techniques improve the strength by almost 200% because of the roughness increase that activates mechanical interlocking. Peel ply improves joint strength of almost 80% due to high roughness induced by its texture. Furthermore, plasma, laser, flame, corona discharge, and chemical functionalization likewise improve the joint strength [120,128]. The effectiveness of plasma in improving the strength is dependent on the carbon/epoxy type [80] and treatment duration [100]. The effectiveness of the flame treatment is dependent on the number of flame passes, *i.e.*, increasing the pass from one to six can double the strength, because the SiO_2 layer and hydroxyl groups developed during the treatment can enhance the surface energy, enabling a strong adhesion with epoxy [29]. The laser was also reported to improve SLJ strength by 300% due to the enhanced roughness and activation of useful functional groups. Chemical functionalization using GO and sGO can increase joint strength by 17%–51% due to the formation of reaction sites for the functional groups to reside and activate at the bonding region [113].

The reduction of strength is generally caused by surface damage and large variations in the surface roughness initiated by manually-driven treatments (sanding, blasting), *e.g.*, the region with low roughness triggers a premature *adhesive failure* in the SLJ specimen [154]. In the peel ply treatment, the degradation of strength is commonly attributed to the fluorine contaminant. The long-duration plasma treatment (30 min) reduced the SLJ strength of carbon/epoxy, because the adherend temperature reaches 135 °C, which damages the surface [100].

Evidently, treatments increase or reduce the strength of the composite single-lap joint. The substantial scatter in SLJ strength may render a difficulty in selecting an appropriate treatment for improving SLJ strength of thermoset composites. This data scatter is also influenced by the strong effect of topological parameters (overlap length, bondline thickness, inner and outer fillet geometry) over the state of stresses within SLJ, which eventually determines the SLJ strength. Nonetheless, we found that controlling parameters in the flame, corona, and laser treatments may guarantee a consistent improvement of SLJ strength in thermoset composites provided that parameter optimization is carried out. Treatments with manual implementation (sanding, blasting) typically yield SLJ strength with considerable disparity. Peel ply may also guarantee a strength improvement if the post-treatment for contaminant removal is performed.

4.2.2. Fracture toughness of composite joints

Fracture toughness (Mode I and Mode II) is the most commonly used mechanical indicator to evaluate the effect of treatments on the mechanical performance. Mode I fracture toughness G_{IC} represents the critical energy required to grow the crack at the bondline or interface upon the application of loading or displacement in the opening mode [155]. Mode II fracture toughness G_{IIC} is a measure of critical energy for the crack growth due to in-plane shear mode [127]. G_{IC} can be obtained by performing double cantilever beam (DCB) test [155], or wedge test [156–158]. Since DCB represents the most widely-used method for G_{IC} measurement in relation with the surface preparation for composites, we discuss only DCB method here. DCB test for composites is usually performed using a flat specimen instead of the tapered one (which is commonly used for metals), and it is calculated using several data reduction methods, namely Modified Beam Theory (MBT), Compliance Calibration (CC), Modified Compliance Calibration (MCC), and Area Method (AM). G_{IIC} is measured using end-notch flexure (ENF) or end-loaded split (ELS), and the data reduction method usually employs Compliance Beam Method (CBM).

Numerous researchers performed DCB and ENF tests to measure G_{Ic} and G_{IIc}, respectively, of composite joints in relation with surface treatments. The effects of various surface treatments on the variation of

Table 6
Reported effects of surface treatment on single-lap joint (SLJ) of composites. The variation in percentage (var. %) is calculated based on the values of untreated specimens.

Treatment	Adherend	Adhesive	Load type	τ_{max} (var. %)	Ref.
Sanding (SiC, 120-grit)	C/E	PBI	T	+180	[80]
Sanding (SiC, 120-grit)	C/E	PBI	T	+14	[80]
Sanding (SiC, 150-grit)	C/E	E	T	+67	[34]
Sanding (SiC, 280-grit)	C/E	E	T	−14	[72]
Sanding (SiC, 320-grit)	C/E	E	3PB	+14	[36]
Sanding (SiC, 320-grit)	C/E	E	T	−16	[139]
Sanding (SiC, 320-grit)	C/E	E	T	−1	[139]
Sanding (SiC, 320-grit)	C/E	E	T	+19	[139]
Sanding (SiC, 320-grit)	C/E	E	T	+102	[139]
Sanding (SiC)	C/E	–	T	+8	[33]
Sanding (80-grit)	C/E	E	T	+28	[81]
Sanding (240-grit)	C/E	E	T	+166	[29,110]
Sanding (-)	C/E	E	T	+67	[119]
Grit blasting (SiC)	C/E	E	T	+5	[132]
Grit blasting (Al_2O_3)	C/E	E	T	+8	[62]
Grit blasting (-)	C/E	–	T	+32	[33]
Soda blasting (-)	C/E	–	T	+36	[33]
Peel ply (PA, S_a = 114.5 μm)	C/E	E	T	+76	[54]
Peel ply (PA, S_a = 16 μm)	C/E	E	T	+30	[54]
Peel ply (PA, S_a = 18.7 μm)	C/E	E	T	+47	[54]
Peel ply (PA, plain)	C/E	E	T	−26	[59]
Peel ply (PA, plain)	C/E	E	T	−50	[59]
Peel ply (PA, plain)	C/E	E	T	−25	[59]
Peel ply (PA, twill)	C/E	E	T	−27	[59]
Peel ply (PA, S_a = 114.5 μm)	G/E	–	T	−36	[54]
Peel ply (PA, S_a = 16 μm)	G/E	–	T	−45	[54]
Peel ply (PA, S_a = 18.7 μm)	G/E	–	T	−39	[54]
Peel ply (polyester)	C/E	E	T	−29	[62]
Peel ply (polyester, S_a = 9.5 μm)	C/E	E	T	−4	[54]
Peel ply (polyester, S_a = 15 μm)	C/E	E	T	+1	[54]
Peel ply (polyester, S_a = 21 μm)	C/E	E	T	+7	[54]
Peel ply (polyester, S_a = 9.5 μm)	G/E	–	T	−55	[54]
Peel ply (polyester, S_a = 15 μm)	G/E	–	T	−52	[54]
Peel ply (polyester, S_a = 21 μm)	G/E	–	T	−50	[54]
Peel ply (polyester, dry)	C/E	E	T	+7	[132]
Peel ply (polyester, wet)	C/E	E	T	+12	[132]
Peel ply (glass)	C/E	E	T	+12	[59]
Peel ply (glass)	C/E	E	T	+31	[66]
Peel ply (-)	C/E	E	T	+17	[61]
Peel ply (-)	C/E	–	T	+36	[33]
Peel ply (-)	G/E	–	T	+39	[61]
Detergent washing	C/E	–	T	+2	[33]
Chem. func. (GO)	C/E	E	T	+17	[113]
Chem. func. (MTES-sGO)	C/E	E	T	+29	[113]
Chem. func. (GPTMS-sGO)	C/E	E	T	+32	[113]
Chem. func. (APTES-sGO)	C/E	E	T	+40	[113]
Chem. func. (APTMS-sGO)	C/E	E	T	+51	[113]
Corona	C/E	–	T	+56	[33]
Corona + Chem. func.	C/E	E	T	+94	[34]
Corona + Chem. func.	C/E	E	T	+57	[34]
Plasma + peel ply	C/E	E	T	−2	[66]
Plasma + sanding	C/E	PBI	T	+14	[80]
Plasma + sanding	C/E	PBI	T	+200	[80]
Flame (pass = 1)	C/E	E	T	+73	[29]
Flame (pass = 6)	C/E	E	T	+131	[29]
Flame (pass = 12)	C/E	E	T	+149	[29]
Laser (CO_2, in atm, 20% layed open)	C/E	E	T	+16	[56]
Laser (CO_2, in atm, 20% layed open)	C/E	E	T	−26	[56]
Laser (CO_2, in atm, 70% layed open)	C/E	E	T	−1	[56]
Laser (CO_2, in atm, 70% layed open)	C/E	E	T	−26	[56]
Laser (CO_2, in CO_2, 20% layed open)	C/E	E	T	−18	[56]
Laser (CO_2, in CO_2, 20% layed open)	C/E	E	T	+14	[56]
Laser (CO_2, in CO_2, 70% layed open)	C/E	E	T	−25	[56]
Laser (CO_2, in CO_2, 70% layed open)	C/E	E	T	−15	[56]
Laser (CO_2, f = 1.20 J/cm^2)	C/E	E	3PB	+35	[36]
Laser (IR)	C/E	–	T	+34	[120]

(*continued on next page*)

G_{Ic} and G_{IIc} (in percentages with respect to the untreated specimens) of carbon/epoxy and glass/epoxy are given in Table 7.

For Mode I, most treatments were reported to improve G_{Ic} with a maximum recorded improvement of up to 1070%. Sanding improves joint toughness by up to a factor of 11×, owing to mechanical interlocking derived from surface roughness of 2–8 μm and the removal of fluorine [34]. Grit blasting generally improves fracture toughness of carbon/epoxy joint provided that the grit size, blasting materials, and distance are properly selected. Gude et al. [63] showed that the

Table 6 (*continued*).

Treatment	Adherend	Adhesive	Load type	τ_{max} (var. %)	Ref.
Laser (UV, f = 0.12 J/cm^2)	C/E	E	T	+233	[119]
Laser (UV, f = 0.24 J/cm^2)	C/E	E	T	+220	[119]
Laser (fiber, f = 0.50 J/cm^2)	C/E	E	T	+109	[129]
Laser (fiber, f = 0.90 J/cm^2)	C/E	E	T	+121	[129]
Laser (fiber, f = 1.78 J/cm^2)	C/E	E	T	+122	[129]
Laser (fiber, f = 2.64 J/cm^2)	C/E	E	T	+250	[129]
Laser (fiber, f = 3.53 J/cm^2)	C/E	E	T	+267	[129]
Laser (fiber, f = 4.43 J/cm^2)	C/E	E	T	+235	[129]
Laser (fiber, f = 5.29 J/cm^2)	C/E	E	T	+206	[129]
Laser (fiber, f = 7.07 J/cm^2)	C/E	E	T	+185	[129]
Laser (fiber, f = 8.84 J/cm^2)	C/E	E	T	+124	[129]
Laser (Nd:YAG, s = 25 μm, 5.6 W, 40 kHz)	C/E	E	T	+12	[132]
Laser (Nd:YAG, s = 25 μm, 5.6 W, 60 kHz)	C/E	E	T	+15	[132]
Laser (Nd:YAG, s = 25 μm, 6.3 W, 30 kHz)	C/E	E	T	+10	[132]
Laser (Nd:YAG, s = 50 μm, 5.6 W, 40 kHz)	C/E	E	T	+15	[132]
Laser (Nd:YAG, s = 50 μm, 5.6 W, 30 kHz)	C/E	E	T	+23	[132]
Laser (Nd:YAG, no aging, 70 °C)	C/E	E	T	−6	[124]
Laser (Nd:YAG, aging 1092 days, RT, 15% RH)	C/E	E	T	+3	[124]
Laser (Nd:YAG, aging 1093 days, 71 °C, 15% RH)	C/E	E	T	−12	[124]
Laser (Nd:YAG, aging 1095 days, 71 °C, 85% RH)	C/E	E	T	−45	[124]
Laser (Nd:YAG, aging 1099 days, RT, 85% RH)	C/E	E	T	−36	[124]

Note: f, fluence; C/E, carbon/epoxy; G/E, glass/epoxy; E, epoxy; T, tension; 3PB, three-point bending; s, spacing.

Table 7
Reported effects of surface treatment on Mode I and Mode II fracture toughness of composites. The variation in percentage (var. %) is calculated based on the values of untreated specimens.

Treatment	Adherend	Adhesive	Mode	Method	G_{Ic} or G_{IIc} (var. %)	Ref.
Sanding (Al_2O_3, 120-grit)	C/E	E	I	MBT	−40	[69]
Sanding (SiC, 150-grit)	C/E	E	I	MBT	+1070	[34]
Sanding (SiC, 280-grit)	C/E	E	I	MBT	−6	[72]
Sanding (-)	C/E	E	I	MBT	0	[126]
Grit blasting (copper)	C/E	E	I	CC	+565	[36]
Grit blasting (Al_2O_3)	C/E	E	I	MBT	+157	[63]
Peel ply (polyester)	C/E	E	I	MBT	−17	[69]
Peel ply (glass)	C/E	E	I	AM	+255	[66]
Etching (acid, HNO_3)	C/E	E	I	MBT	+20	[69]
Etching (base, NaOH)	C/E	E	I	MBT	−81	[69]
Corona + chem. func.	C/E	E	I	MBT	+848	[34]
Corona + chem. func.	C/E	E	I	MBT	+948	[34]
Plasma	C/E	E	I	D5528	+101	[24]
Plasma	C/E	E	I	MBT	+96	[63]
Plasma	G/E	E	I	D5528	−12	[24]
Plasma (pass = 12)	C/E	E	I	MBT	+63	[72]
Plasma (pass = 24)	C/E	E	I	MBT	+81	[72]
Plasma (pass = 24, aging 25 days)	C/E	E	I	MBT	+69	[72]
Plasma (pass = 48)	C/E	E	I	MBT	+88	[72]
Plasma + grit blasting (Al_2O_3)	C/E	E	I	D5528	+66	[24]
Plasma + grit blasting (Al_2O_3)	G/E	E	I	D5528	+77	[24]
Plasma + peel ply	C/E	E	I	AM	+16	[66]
Laser (CO_2, 1.2 J/cm^2)	C/E	E	I	CC	+341	[36]
Laser (CO_2, 3.6 J/cm^2)	C/E	E	I	CC	+94	[36]
Laser (Yb:KYW, 0.12 J/cm^2, 1 mm/s)	C/E	E	I	MBT	+10	[126]
Laser (Yb:KYW, 0.30 J/cm^2, 1 mm/s)	C/E	E	I	MBT	0	[126]
Laser (Yb:KYW, 0.60 J/cm^2, 1 mm/s)	C/E	E	I	MBT	−10	[126]
Laser (Yb:KYW, 0.48 J/cm^2, 5 mm/s)	C/E	E	I	MBT	−20	[126]
Laser (Yb:KYW, 0.42 J/cm^2, 0.1 mm/s)	C/E	E	I	MBT	+12	[126]
Laser (Yb:KYW)	C/E	E	II	CBM	−7[a]	[127]
Laser (Yb:KYW)	C/E	E	II	CBM	−2[a]	[127]
Laser (Yb:KYW)	C/E	E	II	CBM	+11[a]	[127]
Laser (Yb:KYW)	C/E	E	II	CBM	+4[a]	[127]

[a]The exception made to the data, which is compared to the sanded, control specimens.

Note: C/E, carbon/epoxy; G/E, glass/epoxy; E, epoxy; MBT, Modified Beam Theory; CC, Compliance Calibration; MCC, Modified Compliance Calibration; AM, Area Method; BT, Beam Theory; CBM, Compliance Beam Method.

fracture toughness increase is enabled by 220-grit alumina particles blasted at 45° angle and 100–150 mm distance, which yields a surface with 3 μm roughness (with a high density of sharp peaks) and balanced ratio of dispersive-polar surface energies. Blasting using Al_2O_3 improves fracture toughness, as it generates 11 μm roughness, a large quantity of polar functional groups, and removal of Si contaminants [36]. Peel ply improves fracture toughness owing to the improved surface morphology/texture, surface enhanced roughness that enables mechanical interlocking [66], and the increase in surface energy [69]. Acid etching using HNO_3 yields joints with G_{IC} values reaching 1.80 kJ/m^2 (a modest improvement of 20% as compared to the control specimen) owing to a slight enhancement in the surface energy; acid etching does not significantly modify the surface morphology [69]. Chemical functionalization using GPTMS and TetraThiol on carbon/epoxy adherend after corona discharge could improve fracture toughness by 948% and 848%, respectively [34]. The functionalization creates covalent bonds

between the adhesive and substrate, and improves the surface energy of up to 80% [34]. Plasma treatment moderately enhances fracture toughness of carbon/epoxy or glass/epoxy by 10%–90% owing to the improvement in surface energy, surface chemistry (more carboxyl content), and wettability (lower contact angle) [66,63,72]. Plasma can be used as a post-treatment for fracture toughness enhancement after the specimens have been treated using grit blasting [24] or peel ply [66]. Zaldivar et al. [72] suggested to use a short working distance between the plasma probe and treated surface (*e.g.*, 1 mm), high volume of carrier gas, and optimized plasma passes (*e.g.*, 12–24 passes) to improve surface characteristics. Laser treatment modifies the fracture toughness of carbon/epoxy bonded joints depending on the utilized gas, wavelength, laser fluence, and speed [36,126]. The CO^2 laser with 1.2 J/cm^2 fluence achieves higher fracture toughness enhancement than that with 3.6 J/cm^2. A fracture toughness increase of 10% was likewise reported when the Yb:KYW laser was used to treat carbon/epoxy [126].

However, a degradation of G_{Ic} was recorded for almost all treatments due to a variety of reasons. Sanding, peel ply, base etching, plasma, or the Yb:KYW laser degrade G_{Ic} with a highest reduction of up to approximately 80%. The reduction of fracture toughness by sanding is attributed to its manual operation that induces inconsistent roughness [69] and damages in the composite surface [72]. Peel ply degrades fracture toughness due to the trace of contaminants, *e.g.*, fluorine. Etching using NaOH (base solutions) also degrades fracture toughness, as the NaOH is abrasive on the epoxy [69]. Therefore, it is suggested that the epoxy-based composite must not be treated by NaOH etching. Plasma treatment slightly degraded fracture toughness when the plasma setting was not effective in removing the contaminants, *e.g.*, the plasma treatment at 10 mm/s and 6 mm distance is insufficient for the removal of the fluorine from the adherend surface [24]. The CO_2 laser treatment decreases fracture toughness when the laser energy density is set at 3.6 J/cm^2, as it removes epoxy layers from the surface and forms a weak boundary layer due to loose fibers, and poor wetting of adhesive on the bare fibers [36]. A slight modification of fracture toughness was reported when the Yb:KYW laser at high energy density (0.48–0.60 J/cm^2) was used to treat carbon/epoxy due to the full removal of epoxy and fiber damage [126].

For Mode II, effect of surface treatment on G_{IIc} is reported in Refs. [159–161,71,162,163], with the exception of Moreira et al. [127]. In their study [127], the Yb:KYW laser with different levels of energy, speed and laser track distance was used to treat carbon/epoxy for obtaining Mode II fracture toughness via ENF test with reference to the control specimen. They found that laser treatment could produce a contaminant-free surface and larger surface area useful for mechanical interlocking, whereas the G_{IIc} enhancement accounts for merely 11% [127]. A small reduction of G_{IIc} of around 7% was likewise noted. The reduction was caused by contaminants that were not entirely removed by the laser treatment. Nonetheless, a need for studies on the influence of treatments on Mode II performance of thermoset-based composites remains, before solid conclusions are made in this aspect.

5. Toward modern solutions for enhancing joint performances

5.1. Patterning of pre-preg using in-mold method

An in-mold method has been proposed to drastically modify the surface topology of composite substrates [45–47]. This method essentially follows a nanoimprint lithography procedure (depicted in Fig. 7a), introducing periodic step-shaped micro patterns on carbon/epoxy prepreg generated by a corrugated aluminum mold during curing process. Hence, this method is considered applicable for co-cured and co-bonded joints. The SEM image shown in Fig. 7b indicates that the topology of imprinted concave and convex carbon/epoxy structure can be a few times the fiber diameter. Such a micro-pattern introduces a local Mode II fracture region that has high crack resistance into the apparent fracture behavior, as measured by the DCB test (for Mode I) [47] or single leg bending (for mixed Mode I/II) [45]. Consequently, Mode I as well as mixed Mode I/II fracture toughness of the secondary bonded carbon/epoxy joint is improved. In the specimen without micro-patterns, the fracture toughness is relatively low, because the crack is propagating rapidly in a relatively flat adhesive–adherend interface (Fig. 7c). In the specimen with micro-patterns (Fig. 7c), the fracture toughness is enhanced due to a contiguous crack propagation along the corrugated interface. The schematic in Fig. 7d shows that two fracture mechanisms in fact occurred in the specimen with micro-patterns: in one, (i) the crack propagates along the step-shaped micro patterns (interface failure), whereas in the other, (ii) the crack propagates within the adherend and adhesive (cohesive failure). This combination of interface and cohesive failures increases the shear load required to grow the crack (increased local Mode II fracture toughness).

5.2. Patterning of cured laminates using laser irradiation

Recently, the patterning of substrates using laser irradiation has received significant attention. This strategy was found to increase the peel strength of T-joint with metallic substrates, *e.g.*, copper [164–166]. The peel strength was improved, as the energy required to debond the joint was dissipated through cohesive failure and plastic deformation of the metallic substrates [165]. The effect of laser-based surface patterning in composite substrates is provided in the recent studies by Xie et al. [114] (single-lap shear test), Tao et al. [36,37,51] (Mode I fracture), Wagih et al. [163] (Mode II fracture), and Sorrentino et al. [167] (Mode II fracture). This patterning scheme is thus considered applicable for secondary bonded joints.

Xie et al. [114] proposed two-step laser treatment using the Nd:YAG laser on the carbon/epoxy surface, where the first step is aimed to remove the resin layer, such that the carbon fibers can be exposed, and the second step is aimed to produce grooves on the bare carbon fibers (Fig. 8a). As observed using SEM and shown in Fig. 8b, the grooves on composite surface enhance the single-lap shear strength of the cross-ply composite joint of up to 41%, particularly when crossed-groove patterns are employed. The two mechanisms related to the two-step laser treatment were responsible for the shear strength improvement in composite joint with grooves. The first step improves the physical bonding between carbon/epoxy and the adhesive, while the second step introduces an anchoring bonding between carbon/epoxy and the adhesive (Fig. 8c).

Tao et al. [51] employed CO_2 laser irradiation to make an alternating pattern of laser-ablated strips and laser-cleaned strips (Fig. 8d). The laser-ablated strips contained fully exposed carbon fibers, while the laser-cleaned strips contained some matrix that were remained on the surface. This patterning (laser ablation-laser cleaning strategy) triggered the formation of adhesive ligaments at the interface during Mode I fracture test, as shown in Fig. 8e, which were acting as an extrinsic dissipation mechanism. This mechanism was responsible for the final enhancement of R-curve in Mode I, as shown in Fig. 8f. The enhancement of Mode I R-curve was also studied numerically using finite element simulation [50], showing that geometrical factor (gap distance g in Fig. 8d) and contrast between cohesive element parameters (strength, energy) play an important role in the improvement of R-curve. The laser patterning method proposed in Ref. [51] was then adopted by Wagih et al. [163] for treating composite surfaces of ENF specimens (Mode II). Mode II fracture toughness was increased by 60% as compared to the baseline specimen [163]. The underlying mechanism in the Mode II case is different from that of Mode I. In Mode II, the alternating laser patterning on CFRP substrate triggers adhesive cracking and failure as well as crack migration towards other interfaces. These mechanisms dissipate higher energy during crack propagation and improve Mode II fracture toughness of CFRP bonded joint.

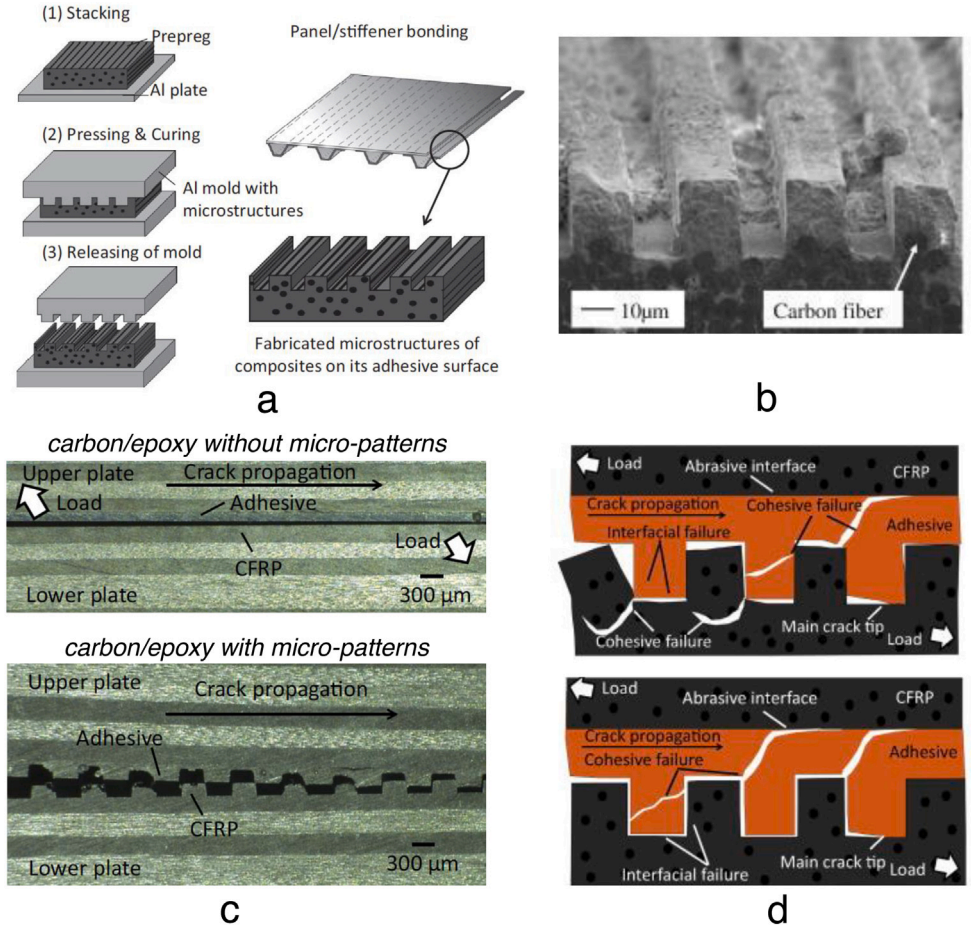

Fig. 7. (a) Schematic of in-mold surface modification by imprint lithography for carbon/epoxy pre-preg [45]; (b) SEM image of carbon/epoxy with imprinted concave and convex structures [47]; (c) crack propagation in carbon/epoxy without and with micro-patterns [45]; (d) schematic of failure mechanisms in carbon/epoxy with micro-patterns [45].

5.3. Tailoring adhesive bondline using inserts/carriers

Although the following methods are not directly related to the surface preparation methods, they have been recently proposed to enhance joint performance. The methods essentially introduce foreign material or layer structures into the adhesive bondline. In some cases adherend surface is also prepared to remove the contaminants, or to create desired roughness. Moreira Arouche et al. [168] inserted a layer of glass fiber chopped strand mat between adherends to enhance the toughness of metal-to-composite joints. Dispersing multi-walled carbon nanotubes or graphene oxide nanoplatelets is also one way to introduce foreign material into the adhesive bondline where fracture toughness of glass/epoxy with aligned nano-fillers can improve Mode I fracture toughness of up to 350% [169]. Since glass fiber or nanofillers are very brittle and delicate, the foreign layer can be selected to be more ductile than the adhesive. As shown in Fig. 9a, Löbel et al. [48] inserted a ductile thermoplastic (polyvenylidene) strip within a rigid adhesive (epoxy) as a crack-stopper in the bondline of CFRP bonded joint, and improved the Mode I fracture toughness locally by 300%. Heide-Jørgensen et al. [49] incorporated a diamond-celled lattice knit (nylon with fiber diameter of 0.4–0.5 mm) into the bondline of CFRP bonded joint with a kissing bond (Fig. 9b). They found that the carrier could recover the fracture toughness after surpassing the kissing bond owing to the bridging nylon ligaments. Fig. 9c shows the schematics of the woven copper mesh and PTFE strip that are inserted in the bondline of the joint. This technique activated bridging ligaments that improve fracture toughness by 250% [52]. Because the layer insert is generally the as-received product without any design freedom, the authors [53] manufactured a carrier with corrugated net-like design using 3D printer (see Fig. 9d), and implemented the carrier in the CFRP bonded joint, where the CFRP substrates were treated by laser ablation (for enhancing the bonding between epoxy and carbon fibers). The authors found that this technique could significantly improve the Mode I fracture toughness of CFRP bonded joints by more than 400%. Extrinsic toughening mechanisms (anchoring and stretching), generated by the micro-architecture inserted in the bondline and the presence of voids in the bondline, are responsible for the toughness improvement [53,170].

5.4. Remarks on the modern solutions

The abovementioned solutions (in-mold method, laser patterning, adhesive tailoring) proposed to enhance the joint performance are still finding their way towards the real, practical applications in a structure. Although laser treatment, for instance, is not yet a practical norm for producing patterns on composite surface (particularly for adhesive bonding purpose), it has been qualified as a technique to remove release agent residues from carbon-fiber reinforced-polymer surface before painting [171]. Laser also has a huge potential to be used as an automated preparation strategy in the manufacture of spacecraft equipment [172]. Similarly, although crack stopper depicted in Fig. 9a (as one of the techniques proposed in European project called BOPACS — Boltless assembling Of Primary Aerospace Composite Structures [173]) may take a huge effort to certify in the aircraft industry, it has some potentials to be incorporated in the secondary bonded joints.

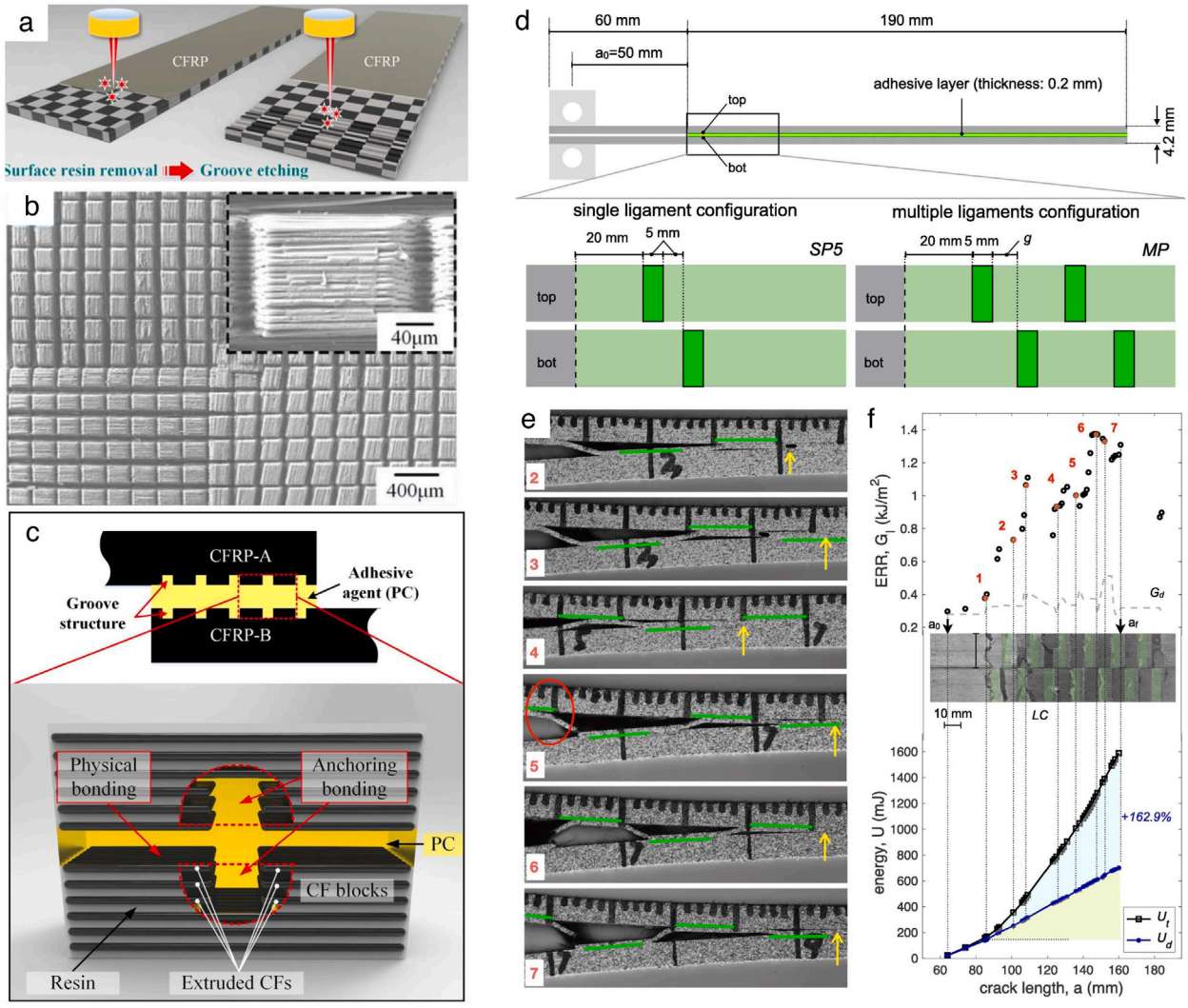

Fig. 8. Laser patterning in single-lap composite joint: (a) schematic of two-step laser treatment, (b) example of SEM image of groove morphology in carbon/epoxy, (c) schematic of mechanisms responsible for shear strength improvement [114]; (d) laser patterning in DCB test specimen for promoting single ligament and multiple ligament, (e) crack propagation in DCB specimen as observed from specimen edge, (f) corresponding energy release rate (ERR), fracture surface, and energy evolution in laser-patterned DCB specimen [51].

6. Conclusions and prospective

Recent progress in the surface preparation strategies for thermoset composites applied in aerospace or automotive industry (carbon/epoxy, glass/epoxy) is critically reviewed in the present study. We report on 11 strategies commonly used for treating carbon/epoxy or glass/epoxy, namely, peel ply, solvent cleaning, detergent washing, sanding, blasting, etching, corona discharge, plasma, flame, laser, and chemical functionalization. We analyzed the effects of these strategies both qualitatively, in terms of adhesion mechanisms/phenomenology, and quantitatively, in terms of surface and mechanical indicators (roughness, contact angle, surface energy, surface chemical composition, joint strength, and fracture toughness).

We found that the following aspects must be considered to select a proper surface preparation: (i) triggering both mechanical interlocking and adsorption/chemical bonding between adhesive and composite adherend, (ii) removal of weak boundary layer due to contaminants — not introducing contaminants or foreign species that are dangerous to the bonding; (iii) viability for industrial scale-up over a large area or complex shape facilitated optimization (*e.g.*, laser, plasma, flame), (iv) improvement of mechanical joint performance. In practice, upon the completion of selected treatment one should first consider the changes in surface morphology, surface roughness, contact angle/wettability, surface energy, surface chemistry, as well as removal of weak boundary layer, as they all contribute to the mechanical interlocking and chemical adhesion of the secondary bonded joints. Thereafter, the final evaluation of treatment can be assessed by mechanical tests (joint strength or toughness measurements). Moreover, we conclude that, albeit important, the remark made in various studies on the relationship between surface preparation and the adhesion mechanism is purely phenomenological, providing limited access to the actual reasons for either strong or weak bonding in secondary bonded composites.

Recent trends show that three modern solutions proposed to enhance joint performance (in-mold method, laser patterning, adhesive tailoring) can be pursued in the future by optimizing the new mechanisms of strengthening/toughening (ligament formation/anchoring). These recent studies introduce a novel paradigm in adhesive bonding, as they highlight the role of imperfections, either random or controlled, in the creation of multiple sub-cracks having a beneficial effect in macroscopic effective toughness.

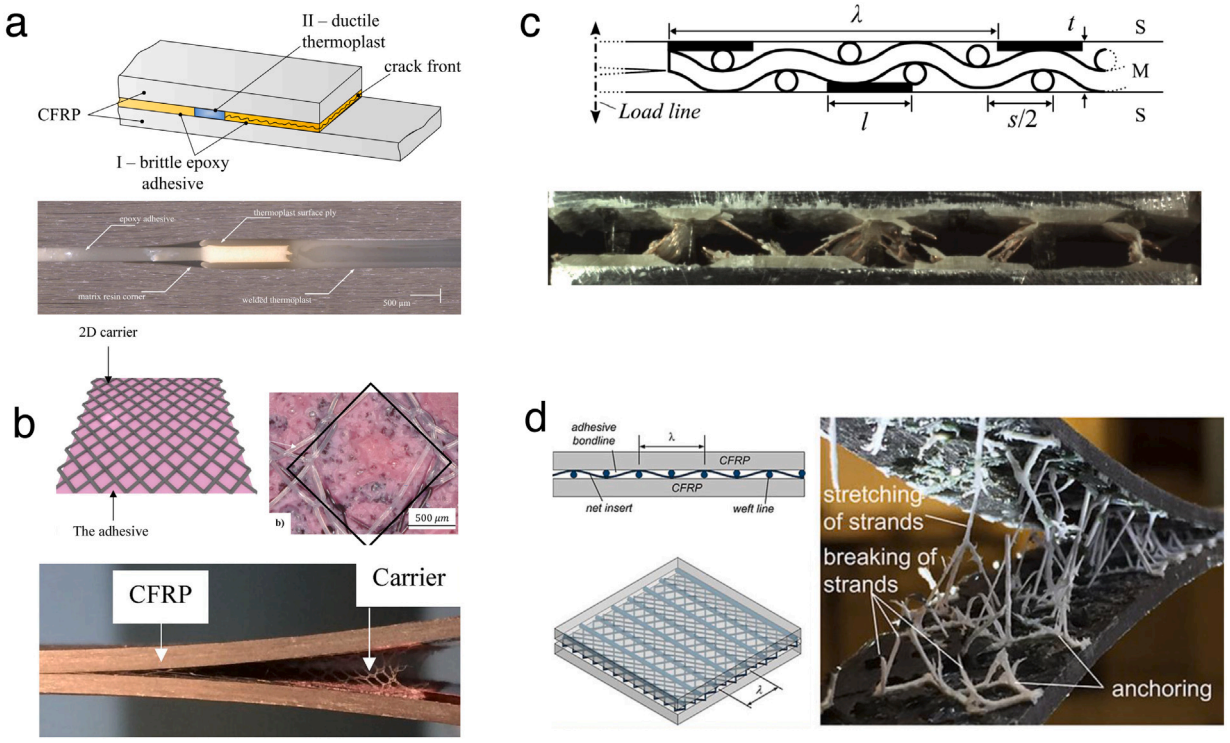

Fig. 9. Methods for creating heterogeneous bondline activating extrinsic toughening by ligaments: (a) ductile thermoplastic inserted as a crack stopper [48], (b) 2D carrier made of nylon [49], (c) copper carrier [52], (d) 3D-printed nylon carrier [53].

Declaration of competing interest

The authors declare that they have no known competing financial interests or personal relationships that could have appeared to influence the work reported in this paper.

Acknowledgments

Funding

This work was supported by the King Abdullah University of Science and Technology (KAUST), Saudi Arabia that provides the Competitive Research Grant (grant number CRG6 2017 3388) and Baseline Research Funds (grant number BAS/1/1315-01-01).

We also thank Dr. Arturo Pascuzzo (UNICAL), Dr. Ran Tao and Dr. Ahmed Wagih (COHMAS Laboratory, KAUST) for discussions and supplying experimental data.

References

[1] Soutis C. Carbon fiber reinforced plastics in aircraft construction. Mater Sci Eng A 2005;412(1):171–6.

[2] Beardmore P, Johnson CF. The potential for composites in structural automotive applications. Compos Sci Technol 1986;26(4):251–81.

[3] Breuer UP. Commercial aircraft composite technology. Springer; 2016.

[4] Niu MCY. Composite airframe structures – Practical design information and data. Conlimit Press Ltd.; 1992.

[5] Messler Jr RW. Joining of materials and structures - From pragmatic process to enabling technology. Elsevier; 2004.

[6] Kaufmann M, Zenkert D, Wennhage P. Integrated cost/weight optimization of aircraft structures. Struct Multidiscip Optim 2010;41(2):325–34.

[7] Bardis J, Kedward K. Effects of surface preparation on the long-term durability of adhesively bonded composite joints (DOT/FAA/AR-03/53). Technical Report January, Santa Barbara: University of California; 2004.

[8] Higgins A. Adhesive bonding of aircraft structures. Int J Adhes Adhes 2000;20(5):367–76.

[9] Davis HO. Secondary bonding of carbon/carbon composites. J Spacecr. Rockets 1979;16(6):432–5.

[10] Kruse T. Bonding of CFRP primary aerospace structures: Overview on the technology status in the context of the certification boundary conditions adressing needs for development. In: The 19th international conference on composite materials, 2013. p. 5635–43.

[11] Whittingham B, Baker AA, Harman A, Bitton D. Micrographic studies on adhesively bonded scarf repairs to thick composite aircraft structure. Composites A 2009;40(9):1419–32.

[12] Röper F, Wolfahrt M, Schlögl S, Kucher G, G Pinter. Bonded aerospace repairs under tensile loading: Wet chemical surface treatment and selected environmental conditions. J Appl Polym Sci 2019;47506:1–9.

[13] Budhe S, Banea MD, de Barros S. Bonded repair of composite structures in aerospace application: A review on environmental issues. Appl Adhes Sci 2018;6(1).

[14] Song MG, Kweon JH, Choi JH, Byun JH, Song MH, Shin SJ, et al. Effect of manufacturing methods on the shear strength of composite single-lap bonded joints. Compos Struct 2010;92(9):2194–202.

[15] Baldan A. Adhesively-bonded joints and repairs in metallic alloys, polymers and composite materials: Adhesives, adhesion theories and surface pretreatment. J Mater Sci 2004;39:1–49.

[16] Banea MD, da Silva LFM. Adhesively bonded joints in composite materials: An overview. Proc Inst Mech Eng L 2009;223(1):1–18.

[17] Rudawska A. Selected aspects of the effect of mechanical treatment on surface roughness and adhesive joint strength of steel sheets. Int J Adhes Adhes 2014;50:235–43.

[18] Ebnesajjad S. Surface treatment of materials for adhesive bonding surface. second ed.. Elsevier Inc.; 2014.

[19] Korta J, Mlyniec A, Uhl T. Experimental and numerical study on the effect of humidity-temperature cycling on structural multi-material adhesive joints. Composites B 2015;79:621–30.

[20] Mlyniec A, Korta J, Uhl T. Structurally based constitutive model of epoxy adhesives incorporating the influence of post-curing and thermolysis. Composites B 2016;86:160–7.

[21] Budhe S, Banea MD, de Barros S, da Silva LFM. An updated review of adhesively bonded joints in composite materials. Int J Adhes Adhes 2017;72:30–42.

[22] Banea MD, da Silva LFM, Carbas RJC, de Barros S. Debonding on command of multi-material adhesive joints. J Adhes 2017;93(10):756–70.

[23] Shang X, Marques EAS, Machado JJM, Carbas RJC, Jiang D, Silva LFM. Review on techniques to improve the strength of adhesive joints with composite adherends. Composites B 2019;177:107363.

[24] Encinas N, Oakley BR, Belcher MA, Blohowiak KY, RG Dillingham, J Abenojar, et al. Surface modification of aircraft used composites for adhesive bonding. Int J Adhes Adhes 2014;50:157–63.

[25] Katnam KB, Da Silva LFM, Young TM. Bonded repair of composite aircraft structures: A review of scientific challenges and opportunities. Prog Aerosp Sci 2013;61:26–42.

[26] Katsiropoulos ChV, Chamos AN, Tserpes KI, Pantelakis SpG. Fracture toughness and shear behavior of composite bonded joints based on a novel aerospace adhesive. Composites B 2012;43(2):240–8.

[27] Thakur S, Neogi S. Tailoring the adhesion of polymers using plasma for biomedical applications: A critical review. Rev Adhes Adhes 2015;3(1):53–97.

[28] Fernholz KD. Bonding of polymer matrix composites. Adv Struct Adhes Bond 2010;3:265–91.

[29] Takeda T, Yasuoka T, Hoshi H, Sugimoto S, Iwahori Y. Effectiveness of flame-based surface treatment for adhesive bonding of carbon fiber reinforced epoxy matrix composites. Composites A 2019;119:30–7.

[30] ASTM-D2093. Standard practice for preparation of surfaces of plastics prior to adhesive bonding. ASTM Book of Standards; 2011, p. 1–3, Reapproved 2017.

[31] Deng S, Djukic L, Paton R, Ye L. Thermoplastic-epoxy interactions and their potential applications in joining composite structures – a review. Composites A 2015;68:121–32.

[32] Park SM, Roy R, Kweon JH, Nam Y. Strength and failure modes of surface treated CFRP secondary bonded single-lap joints in static and fatigue tensile loading regimes. Composites A 2020;134:105897.

[33] Wingfield JRJ. Treatment of composite surfaces for adhesive bonding. Int J Adhes Adhes 1993;13(3):151–6.

[34] Jölly I, Schlögl S, Wolfahrt M, Pinter G, Fleischmann M, Kern W. Chemical functionalization of composite surfaces for improved structural bonded repairs. Composites B 2015;69:296–303.

[35] Chitsaz Dehaghani R, Shokrieh MM, Taheri-Behrooz F. An investigation on effects of acid etching duration on adhesive bonding of polyethylene to E-glass/epoxy composites. Int J Adhes Adhes 2018;85(June):177–83.

[36] Tao R, Alfano M, Lubineau G. Laser-based surface patterning of composite plates for improved secondary adhesive bonding. Composites A 2018;109:84–94.

[37] Tao R, Alfano M, Lubineau G. In situ analysis of interfacial damage in adhesively bonded composite joints subjected to various surface pretreatments. Composites A 2019;116:216–23.

[38] Almuhammadi K, Yudhanto A, Lubineau G. On the anisotropic behavior of electrodes for electrical-based monitoring of CFRP laminated composites. Polym Compos 2019;40(5):2061–6.

[39] Min J, Wan H, Carlson BE, Lin J, Sun C. Application of laser ablation in adhesive bonding of metallic materials: A review. Opt Laser Technol 2020;128(February):106188.

[40] Critchlow GW, Brewis DM. Review of surface pretreatments for aluminium alloys. Int J Adhes Adhes 1996;16:255–75.

[41] Molitor P, Barron V, Young T. Surface treatment of titanium for adhesive bonding to polymer composites: A review. Int J Adhes Adhes 2001;21:129–36.

[42] Carnes MD, Mtenga PV. The effect of materials and surface preparation on joining methods: A review. J Reinf Plast Compos 2015;34(14):1167–78.

[43] Pramanik A, Basak AK, Dong Y, Sarker PK, Uddin MS, G Littlefair, et al. Joining of carbon fibre reinforced polymer (CFRP) composites and aluminium alloys – A review. Composites A 2017;101:1–29.

[44] Fourche G. An overview of the basic aspects of polymer adhesion. Part I: Fundamentals. Polym Eng Sci 1995;35(12):957.

[45] Yukimoto Y, Matsuzaki R, Todoroki A. Effects of mixed-mode ratio and step-shaped micro pattern surface on crack-propagation resistance of carbon-fiber-reinforced plastic/adhesive interface. Composites A 2015;69:139–49.

[46] Suzuki T, Matsuzaki R, Todoroki A, Mizutani Y. Prediction of the macroscopic fracture toughness of a composite/adhesive interface with periodic surface microstructures. Int J Adhes Adhes 2015;60:16–22.

[47] Suzuki T, Matsuzaki R, Todoroki A, Mizutani Y. Crack growth analysis of a composite/adhesive interface toughened by in-mold surface preparation. Int J Adhes Adhes 2013;42:36–43.

[48] Löbel T, Holzhüter D, Sinapius M, Hühne C. A hybrid bondline concept for bonded composite joints. Int J Adhes Adhes 2016;68:229–38.

[49] Heide-Jørgensen S, Teixeira de Freitas S, Budzik MK. On the fracture behaviour of CFRP bonded joints under mode I loading: Effect of supporting carrier and interface contamination. Compos Sci Technol 2018;160:97–110.

[50] Tao R, Li X, Yudhanto A, Alfano M, Lubineau G. On controlling interfacial heterogeneity to trigger bridging in secondary bonded composite joints: An efficient strategy to introduce crack-arrest features. Compos Sci Technol 2020;188:107964.

[51] Tao R, Li X, Yudhanto A, Alfano M, Lubineau G. Laser-based interfacial patterning enables toughening of CFRP/epoxy joints through bridging of adhesive ligaments. Composites A 2020;139:106094.

[52] Maloney K, Fleck N. Toughening strategies in adhesive joints. Int J Solids Struct 2019;158:66–75.

[53] Yudhanto A, Almulhim M, Kamal F, Tao R, Fatta L, M Alfano, et al. Enhancement of fracture toughness in secondary bonded CFRP using hybrid thermoplastic/thermoset bondline architecture. Compos Sci Technol 2020;199:108346.

[54] Bénard Q, Fois M, Grisel M. Peel ply surface treatment for composite assemblies: Chemistry and morphology effects. Composites A 2005;36(11):1562–8.

[55] Kanerva M, Sarlin E, Hoikkanen M, Rämö K, Saarela O, Vuorinen J. Interface modification of glass fibre-polyester composite-composite joints using peel plies. Int J Adhes Adhes 2015;59:40–52.

[56] Hartwig A, Vit G, Dieckhoff S, Hennemann OD. Surface treatment of an epoxy resin by CO2 laser irradiation. Die Angew. Makromol. Chem. 1996;238:177–89.

[57] Tracy J, Yin Y, Yang J, Osborne JC, Blohowiak KY, Dauskardt R. Environmentally assisted crack growth in adhesively bonded composite joints. Composites A 2017;102:368–77.

[58] Kanerva M, Saarela O. The peel ply surface treatment for adhesive bonding of composites: A review. Int J Adhes Adhes 2013;43:60–9.

[59] Holtmannspötter J, Czarnecki JV, Wetzel M, D Dolderer, Eisenschink C. The use of peel ply as a method to create reproduceable but contaminated surfaces for structural adhesive bonding of carbon fiber reinforced plastics. J Adhes 2013;89(2):96–110.

[60] Silveira NNA, Sales RCM, Brito CBG, Cândido GM, Donadon MV. Comparative fractographic analysis of composites adhesive joints subjected to mode I delamination. Polym Compos 2019;40(8):2973–83.

[61] Bénard Q, Fois M, Grisel M. Influence of fibre reinforcement and peel ply surface treatment towards adhesion of composite surfaces. Int J Adhes Adhes 2005;25(5):404–9.

[62] Prolongo SG, Gude MR, Del Rosario G, Ureña A. Surface pretreatments for composite joints: Study of surface profile by SEM image analysis. J Adhes Sci Technol 2010;24(11–12):1855–67.

[63] Gude MR, Prolongo SG, Ureña A. Adhesive bonding of carbon fibre/epoxy laminates: Correlation between surface and mechanical properties. Surf Coat Technol 2012;207:602–7.

[64] Moench MK. The effect of nylon and polyester peel ply surface preparation on the bond quality of composite laminates [Ph.D. thesis], University of Washington; 2013, p. 139.

[65] Zaldivar RJ, Kim HI, Steckel GL, Patel D, Morgan BA, Nokes JP. Surface preparation for adhesive bonding of polycyanurate-based fiber-reinforced composites using atmospheric plasma treatment. J Appl Polym Sci 2011;120:921–31.

[66] Wetzel M, Holtmannspötter J, Gudladt HJ, Czarnecki JV. Sensitivity of double cantilever beam test to surface contamination and surface pretreatment. Int J Adhes Adhes 2013;46:114–21.

[67] Buchmann C, Langer S, Filsinger J, Drechsler K. Analysis of the removal of peel ply from CFRP surfaces. Composites B 2016;89:352–61.

[68] Stoye D. Solvents, encyclopedia of industrial chemistry. Wiley-VCH Verlag GmbH & Co.; 2012.

[69] Martínez-Landeros VH, Vargas-Islas SY, CE Cruz-González, Barrera S, Mourtazov K, Ramírez-Bon R. Studies on the influence of surface treatment type in the effectiveness of structural adhesive bonding for carbon fiber reinforced composites. J Manuf Process 2019;39:160–6.

[70] Wegman RF, Twisk JV. Surface preparation techniques for adhesive bonding. 2nd ed.. Elsevier; 2013.

[71] Mohan J, Ivanković A, Murphy N. Mixed-mode fracture toughness of co-cured and secondary bonded composite joints. Eng Fract Mech 2015;134:148–67.

[72] Zaldivar RJ, Kim HI, Steckel GL, Nokes JP, Morgan BA. Effect of processing parameter changes on the adhesion of plasma-treated carbon fiber reinforced epoxy composites. J Compos Mater 2010;44(12):1435–53.

[73] Underhill PR, Rider AN, DuQuesnay DL. Warm water treatment of aluminum for adhesive bonding. Int J Adhes Adhes 2003;23(4):307–13.

[74] Razavi SMJ, Ayatollahi MR, Nemati Giv A, Khoramishad H. Single lap joints bonded with structural adhesives reinforced with a mixture of silica nanoparticles and multi walled carbon nanotubes. Int J Adhes Adhes 2018;80(October 2017):76–86.

[75] Jhin G, Azari S, Ameli A, Datla NV, Papini M, JK Spelt. Crack growth rate and crack path in adhesively bonded joints: comparison of creep, fatigue and fracture. Int J Adhes Adhes 2013;46:74–84.

[76] Shi J, Bao L, Kobayashi R, Kato J, Kemmochi K. Reusing recycled fibers in high-value fiber-reinforced polymer composites: Improving bending strength by surface cleaning. Compos Sci Technol 2012;72(11):1298–303.

[77] Savage G. Failure prevention in bonded joints on primary load bearing structures. Eng Fail Anal 2007;14(2):321–48.

[78] Davis M, Bond D. Principles and practices of adhesive bonded structural joints and repairs. Int J Adhes Adhes 1999;19:91–105.

[79] Kinloch AJ. Adhesion and adhesives science and technology. Springer-Sci+Bus Media, B.V.; 1987, p. 441.

[80] Iqbal HMS, Bhowmik S, Benedictus R. Study on the effect of surface morphology on adhesion properties of polybenzimidazole adhesive bonded composite joints. Int J Adhes Adhes 2017;72(October 2016):43–50.

[81] Choi I, Lee DG. Surface modification of carbon fiber/epoxy composites with randomly oriented aramid fiber felt for adhesion strength enhancement. Composites A 2013;48(1):1–8.

[82] Yang G, Yang T, Yuan W, Du Y. The influence of surface treatment on the tensile properties of carbon fiber-reinforced epoxy composites-bonded joints. Composites B 2019;160:446–56.

[83] Almuhammadi K, Selvakumaran L, Alfano M, Yang Y, Bera TK, Lubineau G. Laser-based surface preparation of composite laminates leads to improved electrodes for electrical measurements. Appl Surf Sci 2015;359:388–97.

[84] Fernandes RL, De Moura MFSF, Moreira RDF. Effect of temperature on pure modes I and II fracture behavior of composite bonded joints. Composites B 2016;96:35–44.

[85] Boerio FJ, Roby B, Dillingham RG, Bossi RH, Crane RL. Effect of grit-blasting on the surface energy of graphite/epoxy composites. J Adhes 2006;82(1):19–37.

[86] Packham DE. Surface energy, surface topography and adhesion. Int J Adhes Adhes 2003;23(6):437–48.

[87] Alfano M, Lubineau G, Furgiuele F, Paulino GH. Study on the role of laser surface irradiation on damage and decohesion of Al/epoxy joints. Int J Adhes Adhes 2012;39:33–41.

[88] Qi B. Sanding, grit blasting, and plasma etching: Effect on surface composition and surface energy of graphite/epoxy composites [Ph.D. thesis], University of Cincinnati; 2009, p. 146.

[89] Law VJ, Mohan J, O'Neill FT, Ivankovic A, Dowling DP. Air based atmospheric pressure plasma jet removal of FreKote 710-NC prior to composite-to-composite adhesive bonding. Int J Adhes Adhes 2014;54:72–81.

[90] Ramaswamy K, O'Higgins RM, Kadiyala AK, McCarthy MA, McCarthy CT. Evaluation of grit-blasting as a pre-treatment for carbon-fibre thermoplastic composite to aluminium bonded joints tested at static and dynamic loading rates. Composites B 2020;185:107765.

[91] Ayatollahi MR, Nemati Giv A, Razavi SMJ, Khoramishad H. Mechanical properties of adhesively single lap-bonded joints reinforced with multi-walled carbon nanotubes and silica nanoparticles. J Adhes 2017;93(11):896–913.

[92] Marieta C, Schulz E, Irusta L, Gabilondo N, Tercjak A, Mondragon I. Evaluation of fiber surface treatment and toughening of thermoset matrix on the interfacial behaviour of carbon fiber-reinforced cyanate matrix composites. Compos Sci Technol 2005;65(14):2189–97.

[93] Comyn J, Mascia L, Xiao G, Parker BM. Corona-discharge treatment of polyetheretherketone (PEEK) for adhesive bonding. Int J Adhes Adhes 1996;16(4):301–4.

[94] Blackman BRK, Kinloch AJ, Watts JF. The plasma treatment of thermoplastic fibre composites for adhesive bonding. Composites 1994;25(5):332–41.

[95] Goddard JM, Hotchkiss JH. Polymer surface modification for the attachment of bioactive compounds. Prog Polym Sci 2007;32(7):698–725.

[96] Pizzorni M, Lertora E, Mandolfino C. Low pressure plasma treatment of CFRP substrates for adhesive bonding: An investigation of joint durability under severe temperature-moisture conditioning. Int J Adhes Adhes 2020;99:102592.

[97] Adams RD, editor. Adhesive bonding - Science, technology and applications. Woodhead Publishing Limited; 2005.

[98] Zaldivar RJ, Nokes J, Steckel GL, Kim HI, Morgan BA. The effect of atmospheric plasma treatment on the chemistry, morphology and resultant bonding behavior of a pan-based carbon fiber-reinforced epoxy composite. J Compos Mater 2010;44(2):137–56.

[99] Iqbal HMS, Bhowmik S, Benedictus R. Surface modification of high performance polymers by atmospheric pressure plasma and failure mechanism of adhesive bonded joints. Int J Adhes Adhes 2010;30(6):418–24.

[100] Kim JK, Kim HS, Lee DG. Investigation of optimal surface treatments for carbon/epoxy composite adhesive joints. J Adhes Sci Technol 2003;17(3):329–52.

[101] Mandolfino C, Lertora E, Gambaro C. Cold plasma pretreatment of carbon fibre composite substrates to improve adhesive bonding performance. Adv Aerosp Eng 2014;2014:1–7.

[102] Mandolfino C, Lertora E, Gambaro C. Influence of cold plasma treatment parameters on the mechanical properties of polyamide homogeneous bonded joints. Surf Coat Technol 2017;313:222–9.

[103] Baldan A. Adhesion phenomena in bonded joints. Int J Adhes Adhes 2012;38:95–116.

[104] Pizzi A, Mittal KL, editors. Handbook of adhesive technology. 2nd ed.. Marcell Dekker, Inc.; 2003.

[105] Encinas N, Lavat-Gil M, Dillingham RG, Abenojar J, Martínez MA. Cold plasma effect on short glass fibre reinforced composites adhesion properties. Int J Adhes Adhes 2014;48:85–91.

[106] Dighton C, Rezai A, Ogin SL, Watts JF. Atmospheric plasma treatment of CFRP composites to enhance structural bonding investigated using surface analytical techniques. Int J Adhes Adhes 2019;91:142–9.

[107] Cho BG, Hwang SH, Park M, Park JK, Park YB, Chae HG. The effects of plasma surface treatment on the mechanical properties of polycarbonate/carbon nanotube/carbon fiber composites. Composites B 2019;160(August 2018):436–45.

[108] Li W, Xiang D, Wang L, Harkin-Jones E, Zhao C, B Wang, et al. Simultaneous enhancement of electrical conductivity and interlaminar fracture toughness of carbon fiber/epoxy composites using plasma-treated conductive thermoplastic film interleaves. RSC Adv 2018;8(47):26910–21.

[109] Kim JG, Choi I, Lee DG, Seo IS. Flame and silane treatments for improving the adhesive bonding characteristics of aramid/epoxy composites. Compos Struct 2011;93(11):2696–705.

[110] Yasuoka T, Takeda T, Hoshi H, Sugimoto S, Iwahori Y. Wettability, surface geometry and adhesively-bonded joint strength of various surface treatments on titanium alloys or CFRP. Technical report, JAXA-RR-16, JAXA; 2017 [in Japanese].

[111] Rahmani H, Ashori A, Varnaseri N. Surface modification of carbon fiber for improving the interfacial adhesion between carbon fiber and polymer matrix. Polym Adv Technol 2016;27(6):805–11.

[112] Pleşa I, Noţingher PV, Schlögl S, Sumereder C, Muhr M. Properties of polymer composites used in high-voltage applications. Polymers 2016;8(5).

[113] Lee CY, Bae JH, Kim TY, Chang SH, Kim SY. Using silane-functionalized graphene oxides for enhancing the interfacial bonding strength of carbon/epoxy composites. Composites A 2015;75:11–7.

[114] Xie Y, Yang B, Lu L, Wan Z, Liu X. Shear strength of bonded joints of carbon fiber reinforced plastic (CFRP) laminates enhanced by a two-step laser surface treatment. Compos Struct 2020;232:111559.

[115] Fischer F, Kreling S, Dilger K. Surface structuring of CFRP by using modern excimer laser sources. Physics Procedia 2012;39:154–60.

[116] Ohkubo T, Tsukamoto M, Sato Y. Numerical simulation of combustion effects during laser processing of carbon fiber reinforced plastics. Appl Phys A 2016;122(3):1–5.

[117] Hartwig A, Vitr G, Schlett V. Treatment of an epoxy-resin by eximer laser radiation. Int J Adhes Adhes 1997;17(4):373–7.

[118] Bénard Q, Fois M, Grisel M, Laurens P. Surface treatment of carbon/epoxy and glass/epoxy composites with an excimer laser beam. Int J Adhes Adhes 2006;26(7):543–9.

[119] Rauh B, Kreling S, Kolb M, Geistbeck M, Boujenfa S, Suess M, et al. UV-laser cleaning and surface characterization of an aerospace carbon fibre reinforced polymer. Int J Adhes Adhes 2018;82(December 2017):50–9.

[120] Li Y, Zhan X, Gao C, Wang H, Yang Y. Comparative study of infrared laser surface treatment and ultraviolet laser surface treatment of CFRP laminates. Int J Adv Manuf Technol 2019;102:4059–71.

[121] Zhan X, Chen S, Li Y, Wang H, Yang Y. Effect of surface cold ablation on shear strength of CFRP adhesively bonded joint after UV laser treatment. Int J Adhes Adhes 2019;94:13–23.

[122] Zhan X, Li Y, Gao C, Wang H, Yang Y. Effect of infrared laser surface treatment on the microstructure and properties of adhesively CFRP bonded joints. Opt Laser Technol 2018;106:398–409.

[123] Harder S, Schmutzler H, Hergoss P, Freese J, Holtmannspötter J, Fiedler B. Effect of infrared laser surface treatment on the morphology and adhesive properties of scarfed CFRP surfaces. Composites A 2019;121:299–307.

[124] Palmieri FL, Belcher MA, Wohl CJ, Blohowiak KY, JW Connell. Laser ablation surface preparation for adhesive bonding of carbon fiber reinforced epoxy composites. Int J Adhes Adhes 2016;68:95–101.

[125] Akman E, Erdoğan Y, Bora MO, Çoban O, Oztoprak BG, Demir A. Investigation of the differences between photochemical and photothermal laser ablation on the shear strength of CFRP/CFRP adhesive joints. Int J Adhes Adhes 2020;98:102548.

[126] Moreira RDF, Oliveira V, Silva FGA, Vilar R, de Moura MFSF. Influence of femtosecond laser treated surfaces on the mode I fracture toughness of carbon-epoxy bonded joints. Int J Adhes Adhes 2018;82:108–13.

[127] Moreira RDF, Oliveira V, Silva FGA, Vilar R, de Moura MFSF. Mode II fracture toughness of carbon–epoxy bonded joints with femtosecond laser treated surfaces. Int J Mech Sci 2018;148:707–13.

[128] Leone C, Genna S. Effects of surface laser treatment on direct co-bonding strength of CFRP laminates. Compos Struct 2018;194:240–51.

[129] Sun C, Min J, Lin J, Wan H, Yang S, Wang S. The effect of laser ablation treatment on the chemistry, morphology and bonding strength of CFRP joints. Int J Adhes Adhes 2018;84(April):325–34.

[130] Bello I, Alowayed Y, Albinmousa J, Lubineau G, Merah N. Fatigue crack growth in laser-treated adhesively bonded composite joints: An experimental examination. Int J Adhes Adhes 2021;105:102784.

[131] Oliveira V, Sharma SP, de Moura MFSF, Moreira RDF, R Vilar. Surface treatment of CFRP composites using femtosecond laser radiation. Opt Laser Technol 2017;94(November 2016):37–43.

[132] Belcher MA, Wohl CJ, Hopkins JW, Connell JW. Laser surface preparation for bonding of aerospace composites. Proc Inst Civil Eng Eng Comput Mech 2011;164(3):133–8.

[133] Alfano M. Adhesive bonding: Science, technology and applications. Technical report, University of Calabria; 2013.

[134] Awaja F, Gilbert M, Kelly G, Fox B, Pigram PJ. Adhesion of polymers. Prog Polym Sci 2009;34(9):948–68.

[135] Jialanella GL. Advances in bonding plastics. Advances in structural adhesive bonding, No. 3, Woodhead Publishing Limited; 2010, p. 237–64.

[136] Tsiangou E, Teixeira de Freitas S, Fernandez Villegas I, Benedictus R. Investigation on energy director-less ultrasonic welding of polyetherimide (PEI)- to epoxy-based composites. Composites B 2019;173:107014.

[137] Zielecki W, Pawlus P, Perłowski R, Dzierwa A. Surface topography effect on strength of lap adhesive joints after mechanical pre-treatment. Arch Civ Mech Eng 2013;13(2):175–85.

[138] Ramulu M, Wern CW, Garbini JL. Effect of fibre direction on surface roughness measurements of machined graphite/epoxy composite. Compos Manuf 1993;4(1):39–51.

[139] Liu L, Liu X, Kong L, Wang M, Hu P, Wang D. Effect of laser surface treatment on surface and bonding properties of carbon fiber reinforced composites. Int J Mater Form 2019;13:885–95.

[140] Wenzel RN. Resistance of solid surfaces to wetting by water. Ind. Eng. Chem. 1936;28(8):988–94.
[141] Cassie ABD, Baxter S. Wettablity of porous surfaces. Trans. Faraday Soc. 1944;40:546–51.
[142] Rudawska A. Chapter 9 - assessment of surface preparation for the bonding/adhesive technology. In: Rudawska A, editor. Surface treatment in bonding technology. Academic Press; 2019, p. 227–75.
[143] Kreling S, Fischer F, Delmdahl R, Gäbler F, Dilger K. Analytical characterization of CFRP laser treated by excimer laser radiation. Physics Procedia 2013;41:282–90.
[144] ASTM-D5868. Standard test method for lap shear adhesion for fiber reinforced plastic (FRP), vol. 01. ASTM Book of Standards; 2005, p. 4–5, Reapproved 2014.
[145] ASTM-D1876. Peel resistance of adhesives (T-peel test), 08(May). ASTM International; 2015, p. 5–7.
[146] ASTM-D3167. Standard test method for peel resistance of adhesives, vol. 10. ASTM Book of Standards; 2017, p. 1–4.
[147] Teixeira de Freitas S, Sinke J. Test method to assess interface adhesion in composite bonding. Appl Adhes Sci 2015;3(9):1–13.
[148] ASTM-D1781. Standard test method for climbing drum peel for adhesives, vol. 98. ASTM Book of Standards; 2012, p. 1–4.
[149] Moore DR. An introduction to the special issue on peel testing. Int J Adhes Adhes 2008;28(4–5):153–7.
[150] De Sousa CCRG, Campilho RDSG, Marques EAS, Costa M, Da Silva LFM. Overview of different strength prediction techniques for single-lap bonded joints. Proc Inst Mech Eng L 2017;231(1–2):210–23.
[151] Katona TR, Batterman SC. Surface roughness effects on the stress analysis of adhesive joints. Int J Adhes Adhes 1983;3(2):85–91.
[152] Wang CH, Rose LRF. Determination of triaxial stresses in bonded joints. Int J Adhes Adhes 1997;17:17–25.
[153] Wang J, Yao J, Gao H. Specific adhesion of a soft elastic body on a wavy surface. Theor Appl Mech Lett 2012;2(1):014002.
[154] ASTM-D5573. Standard practice for classifying failure mode in fiber-reinforced-plastic (FRP), vol. 99. ASTM Book of Standards; 2012, p. 1–18, Reapproved.
[155] ASTM-D5528. Standard test method for Mode I interlaminar fracture toughness of Unidirectional fiber-reinforced polymer matrix composites, vol. 03. ASTM Book of Standards; 2014, p. 1–12, Reapproved 2007.
[156] ASTM-D3762. Standard test method for adhesive-bonded surface durability of aluminum (wedge test), vol. 03. ASTM Book of Standards; 2010, p. 3–7, Reapproved 2010.
[157] Adams RD, Cowap JW, Farquharson G, Margary GW, Vaughn D. The relative merits of the boeing wedge test and the double cantilever beam test for assessing the durability of adhesively bonded joints, with particular reference to the use of fracture mechanics. Int J Adhes Adhes 2009;29(6):609–20.
[158] Manterola J, Renart J, Zurbitu J, Turon A, Urresti I. Mode I fracture characterisation of rigid and flexible bonded joints using an advanced wedge-driven test. Mech Mater 2020;148:103534.
[159] De Moura MFSF, Campilho RDSG, Gonçalves JPM. Pure mode II fracture characterization of composite bonded joints. Int J Solids Struct 2009;46(6):1589–95.
[160] Ducept F, Davies P, Gamby D. Mixed mode failure criteria for a glass/epoxy composite and an adhesively bonded composite/composite joint. Int J Adhes Adhes 2000;20(3):233–44.
[161] Floros IS, Tserpes KI, Löbel T. Mode-I, mode-II and mixed-mode I+II fracture behavior of composite bonded joints: Experimental characterization and numerical simulation. Composites B 2015;78:459–68.
[162] Pérez-Galmés M, Renart J, Sarrado C, Brunner AJ, Rodríguez-Bellido A. Towards a consensus on mode II adhesive fracture testing: Experimental study. Theor Appl Fract Mech 2018;98(October):210–9.
[163] Wagih A, Tao R, Yudhanto A, Lubineau G. Improving mode II fracture toughness of secondary bonded joints using laser patterning of adherends. Composites A 2020;134(105892).
[164] Hernandez E, Alfano M, Lubineau G, Buttner U. Improving adhesion of copper/epoxy joints by pulsed laser ablation. Int J Adhes Adhes 2016;64:23–32.
[165] Hernandez E, Alfano M, Pulungan D, Lubineau G. Toughness amplification in copper/epoxy joints through pulsed laser micro-machined interface heterogeneities. Sci Rep 2017;7(1):1–12.
[166] Pascuzzo A, Yudhanto A, Alfano M, Lubineau G. On the effect of interfacial patterns on energy dissipation in plastically deforming adhesive bonded ductile sheets. Int J Solids Struct 2020;198:31–40.
[167] Sorrentino L, Marfia S, Parodo G, Sacco E. Laser treatment surface: An innovative method to increase the adhesive bonding of ENF joints in CFRP. Compos Struct 2020;233(111638):1–8.
[168] M. Moreira Arouche, S. Teixeira de Freitas, S. de Barros. On the influence of glass fiber mat on the mixed-mode fracture of composite-to-metal bonded joints. Compos Struct 2021;256:113109.
[169] Gholami R, Khoramishad H, LFM da Silva. Glass fiber-reinforced polymer nanocomposite adhesive joints reinforced with aligned carbon nanofillers. Compos Struct 2020;253:112814.
[170] Heide-Jørgensen S, Budzik MK. Effects of bondline discontinuity during growth of interface cracks including stability and kinetic considerations. J Mech Phys Solids 2018;117:1–21.
[171] Tserpes K. Adhesive bonding of aircraft structures. In: Pantelakis Spiros, Tserpes Konstantinos, editors. Revolutionizing aircraft materials and processes. Springer International Publishing; 2020, p. 337–57.
[172] L.F.M. Da Silva, Öchsner A, Adams RD. Handbook of adhesion technology, volume 2. Springer; 2011, p. 1543.
[173] Halm J. BOPACS (Boltless Assembling of Primary Aerospace Structures). In: The 7th European aernautics day – aerodays 2015. p. 1–14.